Rapid Acquisition of Low Cost High-Resolution Elevation Datasets Using a Small Unmanned Aircraft System: An Application for Measuring River Geomorphic Change

Author: Caleb O. Lucy

Boston College Electronic Thesis or Dissertation, 2015

Boston College

The Graduate School of Arts and Sciences

Department of Earth and Environmental Sciences

RAPID ACQUISITION OF LOW COST HIGH-RESOLUTION ELEVATION DATASETS USING A SMALL UNMANNED AIRCRAFT SYSTEM: AN APPLICATION FOR MEASURING RIVER GEOMORPHIC CHANGE

a thesis

by

CALEB O. LUCY

submitted in partial fulfillment of the requirements for the degree of

Master of Science

December 2015

ABSTRACT

RAPID ACQUISITION OF LOW COST HIGH-RESOLUTION ELEVATION DATASETS USING A SMALL UNMANNED AIRCRAFT SYSTEM: AN APPLICATION FOR MEASURING RIVER GEOMORPHIC CHANGE

Caleb O. Lucy

Advisor: Noah P. Snyder

Emerging methods for acquiring high-resolution topographic datasets have the potential to open new opportunities for quantitative geomorphic analysis. This study demonstrates a technique for rapidly obtaining structure from motion (SfM) photogrammetry-derived digital elevation models (DEMs) using aerial photographs acquired with a small unmanned aircraft system (sUAS). In conjunction with collection of aerial imagery, study sites are surveyed with a differential global position system (dGPS)-enabled total station (TPS) for georeferencing and accuracy assessment of sUAS SfM measurements. Results from sUAS SfM surveys of upland river channels in northern New England consistently produce DEMs and orthoimagery with ~1 cm pixel resolution. One-to-one point measurement comparisons demonstrate sUAS SfM systematically measures elevations about 0.16 ±0.23 m higher than TPS equivalents (0.28 m RMSE). Bathymetric (i.e. submerged or subaqueous) sUAS SfM measurements are 0.20 ±0.24 m (0.31 m RMSE) higher than TPS, whereas exposed (subaerial) points are 0.14 ±0.22 m (0.26 m RMSE) higher than TPS. Serial comparison of DEMs obtained before and after a two-year flood event indicates cut bank erosion and point bar deposition of ~0.10 m, consistent with expectations for channel evolution. DEMs acquired with the sUAS SfM are of comparable resolution but a lower cost alternative to those from airborne light detection and ranging (lidar), the current standard for topographic imagery. Furthermore, lidar is not available for much of the United States and sUAS SfM provides an efficient means

for expanding coverage of this critical elevation dataset. Due to their utility in municipal, land use, and emergency planning, the demand for high-resolution topographic datasets continues to increase among governments, research institutions, and private sector consulting firms. Terrain analysis using sUAS SfM could therefore be a boon to river management and restoration in northern New England and other regions.

TABLE OF CONTENTS

INTRODUCTION

Geomorphology requires high-resolution images and maps of landscape features in order to characterize rates of change. Early studies used small-scale traditional survey and orthophotograph-based topographic maps to describe glacial moraines, drumlins, river meanders, and landslides (e.g., Farrington, 1928; Babenroth and Strahler, 1945; Strahler, 1957). Subsequent digital-age cartography expanded opportunities for quantitative geomorphic analysis. In particular, digital elevation models (DEMs) created from rasterized topographic maps laid the foundation for current models of channel networks, rates of erosion, and tectonic influence on landscape morphology (e.g., Dietrich et al., 1993; Montgomery and Foufoula-Georgiou, 1993; Wobus et al., 2006). The DEMs used in these studies have 10-90 m pixel resolution and are available for most of the Earth's surface.

Contemporary geomorphic studies rely on 1-3 m pixel DEMs created using airborne light detection and ranging (lidar) technology. During these surveys, completed with instrumentation mounted to a large aircraft, laser pulse returns spread across a surface generate a point cloud (i.e. a collection of many points with Cartesian coordinates) that is then interpolated to make a DEM. These newer DEMs cover less of the world's surface than their older equivalents, but permit geomorphic analysis at finer spatial scales that were previously unresolvable. Lidar-based studies have been applied to fault mapping, morphology of postglacial landscapes, changes in river channel morphology, and quantifying aquifer subsidence (e.g., Haugerud et al., 2003; Notebaert et al., 2009; Snyder, 2009; Famiglietti et al., 2011). Ultimately, ever-improving mapping techniques further our understanding of Earth surface processes.

A photogrammetric technique known as structure-from-motion (SfM) has become increasingly utilized for generating high-resolution elevation datasets over the course of the last decade. SfM uses digital photographs to produce a three-dimensional model of a surface that can be converted into a DEM. Traditional stereoscopic photogrammetric techniques use parallax created from two overlapping images of the same scene from different vantage points in order to reconstruct topography (e.g., aerial photograph stereo pairs). SfM, meanwhile, uses numerous (i.e. two or more, often up to 200) photographs from many perspectives that are then input into computer software programs that use pixel-matching algorithms (automatic feature point construction) to produce a point cloud. These digital SfM models can then be georeferenced, exported as DEMs, and imported into a geographic information system (GIS) for further study. Serial comparison of multitemporal DEMs from a landscape enables high-resolution spatial quantification of erosion, deposition, and surficial evolution in that area.

Figure 1. DJI Phantom 2 Vision+ quadcopter, the sUAS used in this study (DJI Innovations, 2014).

Due to relative ease of implementation, low cost, and high data resolution, SfM or photogrammetry-derived elevation measurement has been applied to a wide array of research efforts from a range of disciplines that require detailed topographic information. Aerial photographs from low-altitude surveys with cameras mounted to small unmanned aircraft systems (sUAS, Figure 1) have produced mm-scale DEMs and images of archaeological sites (Eisenbeiss et al., 2005), landslides (Niethammer et al., 2012), dune migration in the North American plains (Hugenholtz et al., 2013), northern New England river channels (Armistead, 2013), and glacial landscape features in Wales (Tonkin et al., 2014).

In particular, the application of sUAS surveys to river research and management has risen over the past few years (Table I). Studies of reaches on braided systems in western North America determine suitability of fish habitat based on analysis of river bathymetry (Tamminga et al., 2014) and the effects of flood events on channel morphology from serial DEM comparison (Tamminga et al., 2015). Other work on meandering systems in Europe focuses on the ability of sUAS SfM to resolve subaqueous portions of river channels in comparison to other measurement methods such as green lidar and multispectral water depth correction (Woodget et al., 2015). Further development of sUAS-based SfM photogrammetry (hereafter sUAS SfM) and its utility in river studies and management serves as motivation for this study.

Table I. Results from previous work applying sUAS SfM to river studies

Study	Approximate sUAS cost ($USD)	Study area extent (km^2)	DEM resolution (m)	Raw vertical RMSE (m)	
				Exposed (subaerial)	Submerged (subaqueous)
(Flener et al., 2013)	3500	0.003	0.05	0.151	N/A
(Lejot et al., 2007)	25000	0.25	0.05-0.10	0.02-0.40*	N/A
(A. D. Tamminga et al., 2015)	60000	0.16	0.05	0.047	0.218
(A. Tamminga et al., 2014)	60000	0.16	0.05	0.088	0.169
(Woodget et al., 2015)	9000	0.01	0.02	0.044*	0.064*
(This study)	*1500*	*0.003-0.025*	*0.01*	*0.26*	*0.31*

*Average error

The objectives of this study are: (1) implement sUAS SfM at several sites in New Hampshire, USA where geomorphic change is expected to occur, particularly in dynamic channels in the upper Saco River watershed (Table II); (2) establish the accuracy and precision of sUAS SfM in comparison with a differential global position system (dGPS)-enabled total station (TPS) surveys conducted simultaneously with sUAS SfM surveys; (3) determine inherent errors and limitations of sUAS SfM and how they might be overcome; and (4) use the results of sUAS SfM to measure geomorphic change at the study sites.

METHODS

Study sites

I surveyed three reaches on the Souhegan, Rocky Branch and Wildcat rivers in New Hampshire, USA (Tables II-III; Figure 2). I also surveyed a site on the main stem Saco River ~10 km downstream of the Rocky Branch site, but sUAS SfM reconstruction for this site could not be completed due to insufficient photographic data; however, these TPS survey results were still used for error analysis of survey data. Because the study sites are subject to both anthropogenic influences and recent floods, they likely experience short-term (<1 year) geomorphic change and therefore well suited to this study. Like many other New England rivers, humans have significantly altered these channels since Colonial settlement in the latter half of the seventeenth century. Channel modification continues into the present, particularly in reaches on the Rocky Branch and Wildcat that were affected by historic flooding during Tropical Storm Irene in August 2011 (Stampone, 2011) and following the removal of the Merrimack Village Dam (MVD) directly downstream of the Souhegan site (Pearson et al., 2011). Since recording began in 1904, two of the ten largest flood events in the upper Saco River watershed (the larger drainage containing the Rocky Branch and Wildcat rivers) have occurred within the past five years (Table IV).

Methodology overview

Combined sUAS SfM and TPS surveys were conducted on the Rocky Branch, Souhegan, and Wildcat rivers during the summer of 2014 in low discharge conditions to ensure maximum subaerial exposure of channel morphology and low water turbidity. A number of different instruments and associated methods were used in this experiment in order to measure geomorphic change at the study sites (Figure 3). First, TPS data collected during sUAS SfM surveys were analyzed to assess baseline survey accuracy. The sUAS SfM survey data were then processed using two different software workflows and analyzed with a variety of statistical techniques in order to determine error and accuracy of final sUAS SfM survey data. Finally, I surveyed the Rocky Branch and Wildcat River sites again in May 2015 using only sUAS SfM and used additional software in to measure geomorphic change at these sites during the year since the initial surveys.

Table II. Study sites

River	Absolute site location	Town	Approximate drainage area (km^2)	Length of reach surveyed (m)	Nearest USGS gauging station (ID)
Rocky Branch	44.104°N, 71.199°W	Glen, NH	40	150	Conway, NH (01064500)
Souhegan	42.858°N, 71.495°W	Merrimack, NH	450	275	Souhegan, NH (01094000)
Wildcat	44.188°N, 71.193°W	Jackson, NH	25	75	Conway, NH (01064500)

Table III. sUAS SfM survey details

	sUAS SfM survey site, area							
	Rocky Branch, 0.005 km^2				Wildcat, 0.003 km^2			
Aerial photograph geometry	Survey date	Number of photographs	Lighting	Imagery resolution (m)	Survey date	Number of photographs	Lighting	Imagery resolution (m)
Normal to ground surface (traditional)	-	-	-	-	June 25, 2014	70	diffuse	0.0091
Normal to ground surface (traditional)	July 14, 2014	56	diffuse	0.0082	July 14, 2014	43	diffuse	0.0084
Normal and oblique to ground surface (convergent)	May 26, 2015	61	direct	0.0104	May 27, 2015	40	direct	0.0099

	Souhegan, 0.025 km^2			
Aerial photograph geometry	Survey date	Number of photographs	Lighting	Imagery resolution (m)
Normal to ground surface (traditional)	July 21, 2014	158	direct	0.0144

Table IV. Top ten recorded annual maximum flood events in the Upper Saco River Watershed

Event rank	Year	Peak discharge (m^3s^{-1})	*RI* (yr)
1	2011	1648	91.0
2	1953	1337	45.5
3	1987	1320	30.3
4	1936	1260	22.8
5	1960	1240	18.2
6	1977	1147	15.2
7	1998	1034	13.0
8	1973	991	11.4
9	1951	929	10.1
10	2014	878	9.1

Discharge recorded on the Saco River near Conway, New Hampshire from water years 1904 to 2014, ranked by annual peak discharge with event year and recurrence interval (*RI*). No records exist from 1910-29. The largest (2011) event was Tropical Storm Irene (U.S. Geological Survey, 2015).

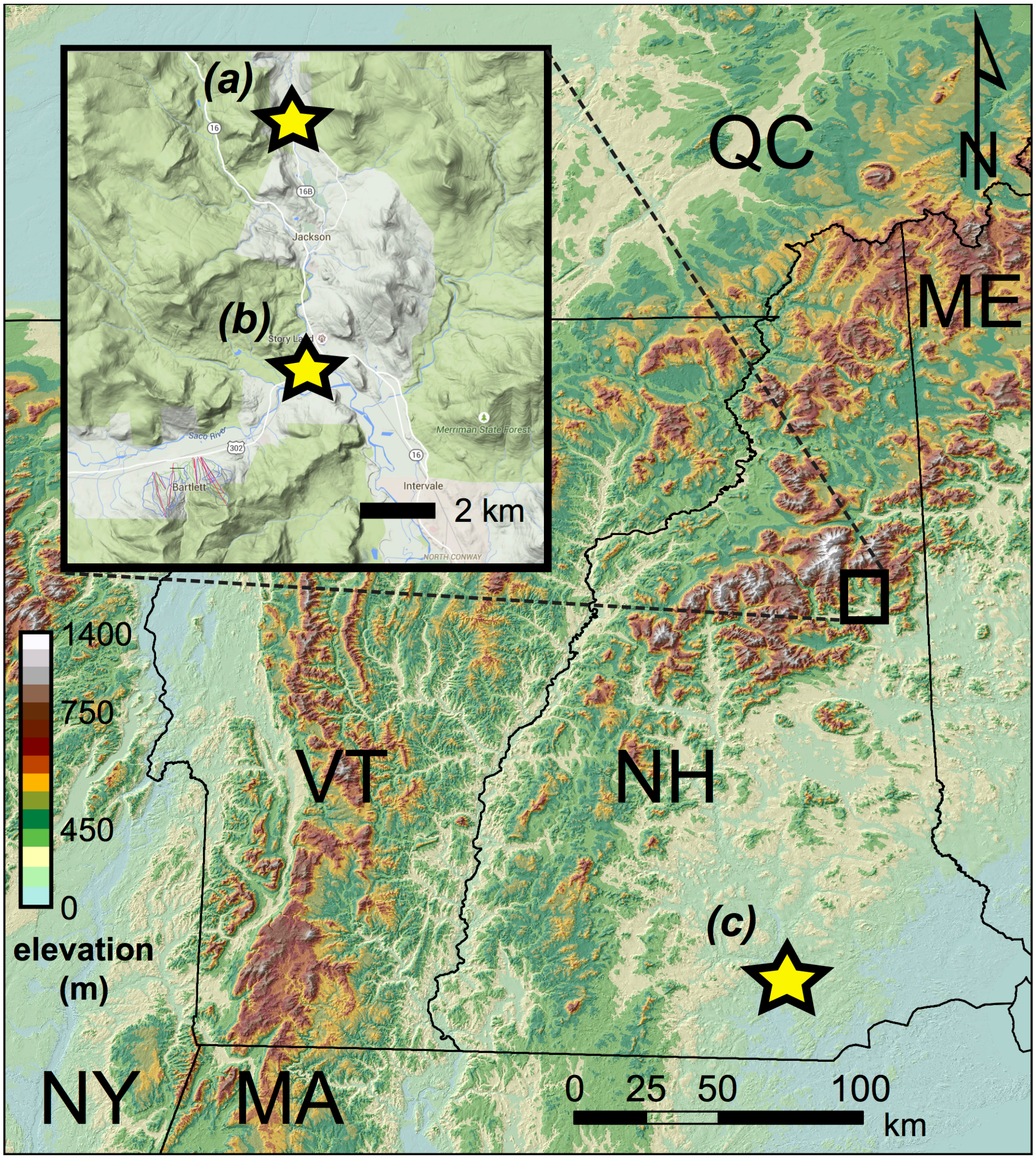

Figure 2. Map of northern New England field sites used in this study: (inset) Wildcat River (a); Rocky Branch (b); and Souhegan River (c) (inset base map from Google, Inc.).

TPS surveys and GCP placement

Surveying with a modern theodolite is an established, widely used measurement method in fluvial geomorphology (e.g., Lane et al., 1994; Merritts et al., 1994; Keim et al., 1999; Pearson et al., 2011; Bangen et al., 2014). In this approach, a total station is used to measure the latitude, longitude, and elevation (XYZ coordinates) of points distributed over a given site. Interpolation of these points using GIS creates a triangulated irregular network (TIN), which can then be rasterized to produce a DEM. The more survey points collected, the higher the resolution of the resulting DEM will be, but each survey point must be collected individually. Creating a high-resolution DEM using the traditional survey method is therefore time and labor intensive.

In this study, I measured ground control points (GCPs) and cross sections using traditional survey methods for one-to-one comparison with SfM estimates of equivalent points. Each study site was surveyed with a global position system (GPS)-enabled Leica TCR 1201 total station (TPS) with mm-scale relative accuracy in conjunction with several sUAS SfM surveys during the summers of 2014 and 2015. A minimum of two cross sections were surveyed at every site, with each of these cross sections measured relative to a different TPS setup, except at the Souhegan site where two cross sections (MVD03 and MVD04) were measured from one total station setup. A minimum of two GPS setups was necessary to convert TPS measurements into absolute coordinates and these stations were backsighted to each other in the field. The GPS data collected at each base station were then post-processed using the Online Positioning User Service (OPUS). OPUS is a web-based service run by the United States' National Geodetic Survey (NGS) that provides differentially corrected GPS positions based on a network of geodetic-quality continuously operating reference stations (CORS) as part of the National Spatial Reference System (Stone, 2006). By processing survey data with OPUS, I ensured best practice for absolute measurement of cross sections and GCPs (Appendix). Similar accuracy surveys could be produced using real-time kinematic GPS equipment at many sites.

Whereas upstream and downstream cross sections were newly created at the Rocky Branch and Wildcat sites in 2014, those at the Souhegan site were transects established in 2007 as part of an ongoing river restoration and monitoring project. These three cross sections have been measured about once a year since 2007 in order to evaluate river channel change following the 2008 removal of the Merrimack Village Dam (Pearson et al., 2011). Cross section survey point spacing ranged from 25 to 50 cm and the transects were 25 to 100 m in length.

I placed GCPs throughout the sites at an even distribution of approximately 4 per 1000 m^2. GCPs were measured with the TPS and used to georeference DEMs generated from sUAS SfM. GCPs were established on prominent immobile objects within each site (i.e. cross section pin tops and boulder crests) that could easily be identified in photographs and selected during georeferencing. Setting up such an absolute ground control framework (GCF) requires only one TPS survey per site and reduces subsequent surveys to only an aerial element taking approximately 20 minutes. GCFs therefore minimize data collection time for multitemporal sUAS surveys and allow for rapid acquisition of photogrammetry-derived high-resolution elevation datasets.

sUAS SfM surveys

Photographs for the SfM surveys conducted during this study were acquired with a DJI proprietary Phantom Vision FC200 camera mounted to highly maneuverable DJI Phantom 2 Vision+ quadcopter (sUAS hereafter) with ~25 minute flight time (DJI Innovations, 2014). The FC200 camera has a focal length of 5 mm and 105° field of view (FOV) with a 6.17 × 4.55 mm (1/2.3") sensor capable of acquiring 16-bit true-color RGB (red, green, blue) images with a resolution of 14 megapixels (4384 × 3288) that are saved in DNG format on a data card onboard the sUAS. The sUAS was used to take photographs normal (nadir) and oblique to ground surface along flight paths approximately 50 m above the ground surface within sight and under control of a human operator (e.g., Fonstad et al., 2013; Johnson et al., 2014). Similar studies used preprogrammed flights paths, but the sUAS used in this study is not equipped with such a feature.

It is important to note that due to the small focal length and wide field of view of the DJI camera, all images are distorted and, if left uncorrected, unusable for SfM reconstruction. The DJI camera has a pronounced barrel distortion, or "fisheye effect", characterized by radial warping that causes shortened pixel mapping with increasing distance from the center of the image (Hugemann, 2010). Essentially, a circular horizon surrounds the image with points becoming progressively more distorted nearer to that edge. The Adobe Lens Profile software plugin (within the Photoshop computer program) corrects a distorted image based on the focal length of the lens used to acquire that image (DJI Innovations, 2014). The Lens Profile for the Phantom Vision FC200 camera filters the digital photograph and restores it to an undistorted raster, allowing SfM reconstruction from images taken with the DJI camera.

The first method used for generating an sUAS SfM elevation dataset (hereafter Method 1) begins by importing corrected images into Photoscan (Agisoft LLC, St. Petersburg, Russia) SfM photogrammetry suite, that (1) generates a SfM model by aligning images; (2) creates a dense point cloud from pixels common to multiple images with bundle block adjustment-based photogrammetry algorithms; and (3) uses the calculated point cloud to create a dense three-dimensional mesh (Figures 3 and 4). I used default processing settings within Photoscan, georeferenced each SfM reconstruction with GCP coordinate data from TPS surveys, and exported the SfM models as DEMs and mosaic orthoimagery to the ArcGIS geospatial software program (Environmental Systems Research Institute, Inc., Redlands, California) for further processing. Each reconstruction used approximately 50 photographs and took approximately 24 hours to create with the bulk of this time (23 hours) consisting of autonomous computer processing.

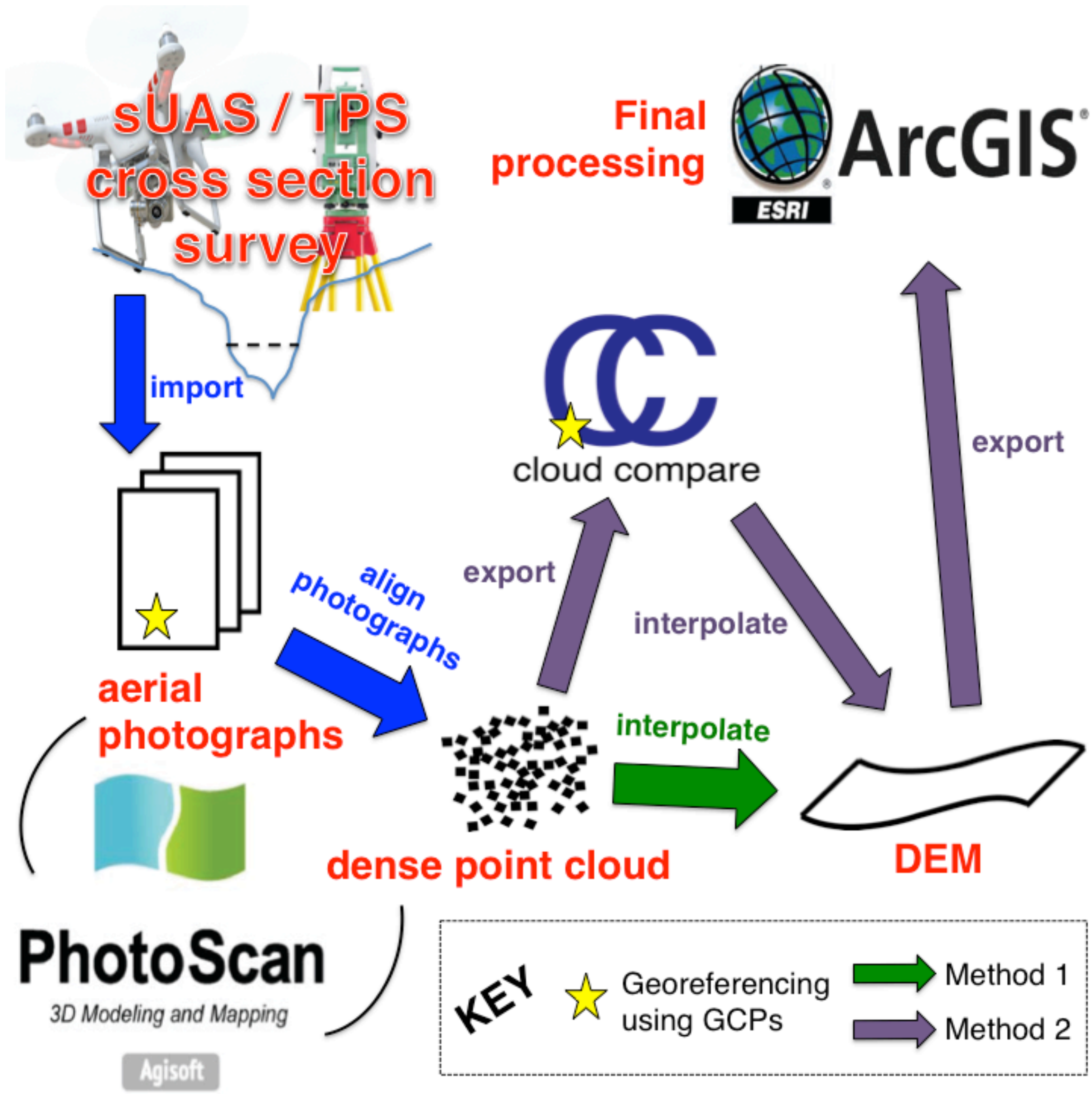

Figure 3. A workflow diagram summarizing how sUAS SfM data are processed using different methods (Methods 1 and 2). Both methods use sUAS/TPS survey data processed in Photoscan to produce a dense cloud 3D model of the survey surface but diverge after this step: whereas Method 1 creates a DEM from sUAS SfM model data processed entirely within Photoscan, Method 2 uses CloudCompare to georeference and interpolate the dense cloud and interpolate to create a DEM. DEMs from both Methods 1 and 2 are exported to ArcGIS.

A second method (hereafter Method 2) for generating DEMs used the dense point cloud generated during step (2) in Method 1, which was then imported into the CloudCompare point cloud processing computer program. In CloudCompare, the imported sUAS SfM survey point cloud was (1) georeferenced by manually aligning it with the point cloud created by TPS survey data; (2) converted to a three-dimensional mesh; (3) exported as a DEM to ArcGIS for further processing (Figure 3). Although each reconstruction processed using Method 2 used the same number of photographs as Method 1 (50), reconstructions took about 27 hours to process due to additional point cloud manipulation in software external to PhotoScan (approximately 24 hours of autonomous computer and 3 hours of user-guided processing).

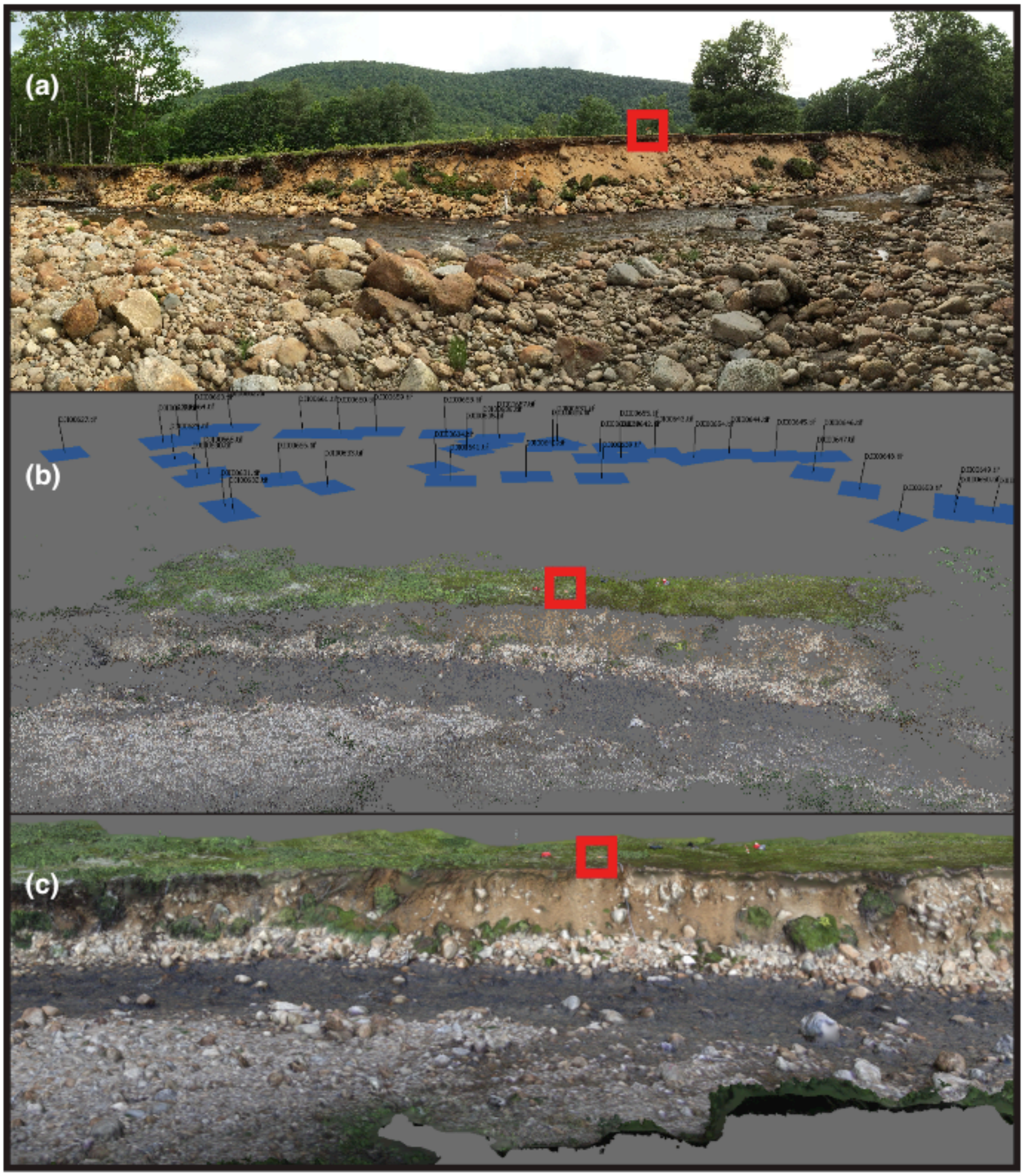

Figure 4. Image (a) is a panoramic photograph of the Wildcat River study site, marked with a GCP (red square) for a SfM survey. Image (b) shows an SfM point cloud model of the outcrop created by the AgiSoft Photoscan computer program using a collection of aerial photographs of the site with the calculated camera positions for these photographs indicated by the blue rectangles in the image. Image (c) shows the surface model of the outcrop created from the interpolation of the SfM point cloud.

Survey accuracy, bias and precision

Although the TPS instrument was rated to mm-scale relative accuracy, I tested its ability to reliably measure the absolute horizontal (XY) and vertical (or elevation, Z) position of a given point by comparing sets of equivalent point measurements. As explained previously, I first evaluated GPS-induced survey errors using OPUS (Table V). Next, I tested the ability of the TPS to consistently determine the location a given point (i.e. TPS measurement reproducibility) by surveying the same point twice from different intrasurvey TPS setup locations. By comparing the base TPS survey data used for georeferencing the photogrammetrically-derived sUAS SfM survey model in PhotoScan with their equivalent positions from the resulting SfM DEM, I then established the vertical accuracy of sUAS SfM survey data. Finally, one-to-one equivalent vertical point comparisons of TPS to sUAS SfM cross section survey measurements were conducted for rigorous evaluation of sUAS SfM survey accuracy. In summary, I used a combination of accuracy (RMSE), bias (average offset or mean error, ME) and precision (standard deviation, SD) to evaluate the following survey measurement components: (1) OPUS-corrected GPS absolute TPS station location data, (2) repeat, inter-station TPS measurement of survey points (e.g. GCPs), (3) GCP measurements by TPS compared with elevation derived from sUAS SfM-derived DEM, and (4) cross-section measurements by TPS compared with sUAS SfM (Walther and Moore, 2005).

Measuring geomorphic change

In order to measure geomorphic change, DEMs generated from 2015 surveys were compared to those from 2014 at the Rocky Branch and Wildcat study reaches.

Similar studies using photogrammetrically-derived DEMs of fluvial environments implement simple raster subtraction to generate a DEM showing elevation changes in a certain area over a given amount of time. This comparative raster is called a DEM of difference (DoD) and displays where sediment erosion and deposition have occurred within the study area. Due to uncertainties in data sources, creation, and rendering of DEMs, however, it is difficult to separate actual geomorphic change (signal) from artificial change (noise), and/or differences in the DEM introduced by survey or geoprocessing errors. Research focusing on minimizing temporally and spatially variant error in serial DEM comparison is called geomorphic change detection (GCD) and better quantifies erosion, deposition, or no change in the river channel (or other dynamic landscape). A Geomorphic Change Detection plugin (Wheaton et al., 2010) for ArcGIS was used to determine rates of erosion and deposition. Wheaton et al. (2010) provide a full documentation of GCD research.

RESULTS

Survey error analysis

Orthophotographs and DEMs from initial sUAS SfM surveys from surveys sites have a pixel resolution of 0.01 m (e.g. Figure 5) with few artifacts or reconstruction inconsistencies evident upon visual inspection. An evaluation of these results begins with an assessment of GPS data collected from 8 base station setups (two setups per site including the Saco River) by the TPS and corrected via OPUS: these measurements had a root-mean-square error (RMSE) of 0.007 ±0.003 m, 0.005 ±0.002 m, and 0.036 ±0.028 m for X (easting), Y (northing), and elevation (Z), respectively (Table V). At 3.6 cm, the vertical error was about five times greater in magnitude than that for horizontal measurement with a greater standard deviation. These GPS errors are the baseline for absolute error of TPS measurements.

Table V. OPUS-derived GPS errors

Survey site	TPS station	Cross section(s) measured	Root-mean-square error (RMSE)		
			Easting (m) UTM 19N	Northing (m) UTM 19N	Elevation (m) NAVD88
Rocky Branch	1	downstream	0.007	0.005	0.017
	2	upstream	0.009	0.004	0.030
Saco River	1	upstream	0.007	0.011	0.100
	2	downstream	0.008	0.006	0.027
Souhegan River	1	MVD03, MVD04	0.004	0.004	0.019
	2	MVD05	0.014	0.004	0.044
Wildcat River	1	downstream	0.005	0.004	0.034
	2	upstream	0.005	0.004	0.015
n = 8		*Average*	*0.007*	*0.005*	*0.036*
		Standard deviation	*0.003*	*0.002*	*0.028*

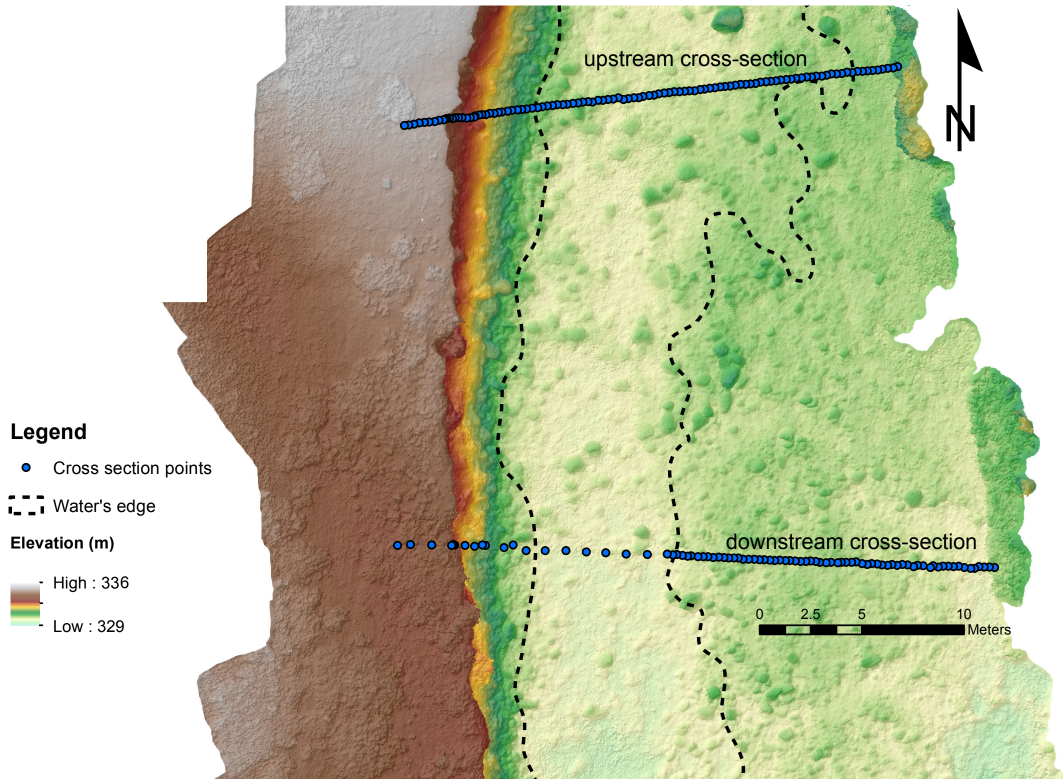

Figure 5. DEM (with 1 cm pixel resolution) generated from the combined sUAS SfM and TPS survey of the Wildcat River study site in Jackson, NH on July 14, 2014.

Repeated inter-station TPS measurement consisted of 18 equivalent point measurements (i.e. the same point measured twice, from two separate base-stations setups, within a given survey). Again, these measurements came from four surveys, one conducted at each of the three main study areas plus one at a location on the main stem Saco River. Results show that RMSE of XYZ position measurement by the TPS was 0.0300 ±0.0013 m, 0.0304 ±0.0013 m, and 0.0418 ±0.0022 m, respectively (Table VI). Using these methods, these results show that the TPS instrument is capable of measuring the absolute position of survey points within 3-4 cm— this represents the error associated with the GCPs used to georeference the sUAS survey data.

Table VI. TPS survey errors

Survey site	Point	Intrasurvey measurement difference (station 1 – station 2) Easting (m) UTM 19N	Northing (m) UTM 19N	Elevation (m) NAVD88
Rocky Branch	GCP 1	0.0096	0.0105	-0.0673
	GCP 2	0.0170	0.0394	-0.0809
	GCP 3	0.0068	-0.0168	-0.0706
Saco River	Top of left pin, downstream cross section	0.0228	0.0332	0.0617
	Top of right pin, downstream cross section	-0.0223	0.0050	0.0463
	Top of left pin, upstream cross section	-0.0056	-0.0139	0.0573
	Top of right pin, upstream cross section	-0.0389	-0.0346	-0.0009
	Downstream GCP	-0.0033	0.0106	0.0648
Souhegan River	GCP 1	-0.0174	0.0244	-0.0203
	GCP 2	0.0630	-0.0125	-0.0141
	GCP 4	-0.0077	0.0058	-0.0110
	GCP 5	-0.0032	0.0547	0.0035
Wildcat River	GCP 1	0.0481	0.0684	-0.0172
	GCP 2	0.0181	0.0249	-0.0100
	GCP 3	-0.0610	-0.0007	-0.0149
	GCP 4	0.0468	0.0477	-0.0083
	Top of left pin, upstream cross section	-0.0033	0.0265	-0.0194
	Top of right pin, upstream cross section	0.0164	0.0033	-0.0098
n=18	*Standard deviation (SD)*	*0.0013*	*0.0013*	*0.0022*
	Root-mean-square error (RMSE)	*0.0300*	*0.0304*	*0.0418*

After extracting point elevations from the photogrammetrically-derived DEMs, one-to-one point comparisons between the sUAS SfM and TPS elevation datasets were processed and rendered using MATLAB (The MathWorks, Inc., Natick, Massachusetts). A comparison of 19 georeferenced GCP elevations from the Rocky Branch, Souhegan, and Wildcat rivers showed the TPS and sUAS SfM-derived GCP elevations had a average offset (ME) of 0.002 ±0.205 m (SD) with an RMSE of 0.200 m (Table VII). DEMs georeferenced in Photoscan do not faithfully reproduce elevations input into them during the georeferencing process, a recognized problem with Photoscan that has yet to be resolved (stihl, 2014). However, sUAS SfM DEMs from the smaller Rocky Branch and Wildcat sites reproduced GCP elevations more faithfully (on the order of 10 cm) than the larger Souhegan site (13-48 cm). Overall, Photoscan produced sUAS SfM DEMs with georeferencing that has equal accuracy and precision on the order of 20 cm.

Table VII. GCP errors

Survey site	Point	TPS survey elevation (m) NAVD88	sUAS SfM elevation (m) NAVD88	sUAS – TPS elevation difference (m)
Rocky Branch	GCP 1	174.172	174.158	0.014
	GCP 2	173.552	173.561	0.008
	GCP 3	172.979	172.986	0.007
	Top of right pin, Upstream cross section	174.184	174.083	-0.101
	TPS survey station 1	173.619	173.724	0.105
	Downstream GCP	173.368	173.378	0.010
Souhegan River	GCP1	34.464	34.788	0.324
	GCP2	34.752	35.234	0.482
	GCP3	35.426	35.231	-0.195
	GCP4	34.255	34.382	0.128
	GCP5	34.260	34.438	0.178
	GCP6	35.258	34.972	-0.286
Wildcat River	GCP 1	331.090	331.067	-0.026
	GCP 2	330.639	330.643	0.004
	GCP 3	330.786	330.799	0.013
	GCP 4	330.403	330.435	0.032
	Top of left pin, downstream cross section	330.580	330.258	-0.322
	Top of right pin, downstream cross section	333.489	333.135	-0.353
	TPS survey station 1	334.964	335.012	0.048
	n=19		*Average (ME)*	*0.002*
			Standard deviation (SD)	*0.205*
			Root-mean-square error (RMSE)	*0.200*

A total of seven cross sections were surveyed at the Rocky Branch, Souhegan, and Wildcat river sites in July 2014 and one-to-one differences in elevation values between survey points obtained using TPS and sUAS SfM surveys were plotted and analyzed (Figures 6-8; Table VIII). In general, Method 1 (georeferencing within Photoscan) measurements were more consistent with TPS measurements than their Method 2 (georeferencing in CloudCompare) equivalents. Elevation measurements by sUAS SfM survey were systematically higher than TPS equivalents and surveys by sUAS SfM at the smaller sites (Rocky Branch and Wildcat) produced more accurate results than surveys done at the larger Souhegan River site (Figures 6-8; Table VIII). The most accurate (lowest average difference and RMSE) and precise (lowest standard deviation) site-wide sUAS SfM survey was at the Rocky Branch site, which measured elevations 0.069 ±0.129 m with a RMSE of 0.145 whereas the least accurate and precise was at the Souhegan site, which measured 0.284 ±0.295 m with a RMSE of 0.409.

Measurements of submerged (subaqueous) topography using sUAS SfM were less accurate and precise than exposed (subaerial) topography (Table VIII). In general, bathymetric surveys (i.e. submerged points) by sUAS SfM systematically measured elevations higher than TPS, but with a greater offset (less accurate and less precise). The only sUAS SfM survey that measured points lower than TPS was the submerged portion of the MVD03 Souhegan cross section survey (22 points), which showed a sUAS SfM - TPS difference of -0.079 ±0.140 m with a RMSE of 0.158. Because Method 1 measures elevation more accurately and precisely than Method 2, I used Method 1 for further sUAS SfM data processing and report results using only Method 1 hereafter.

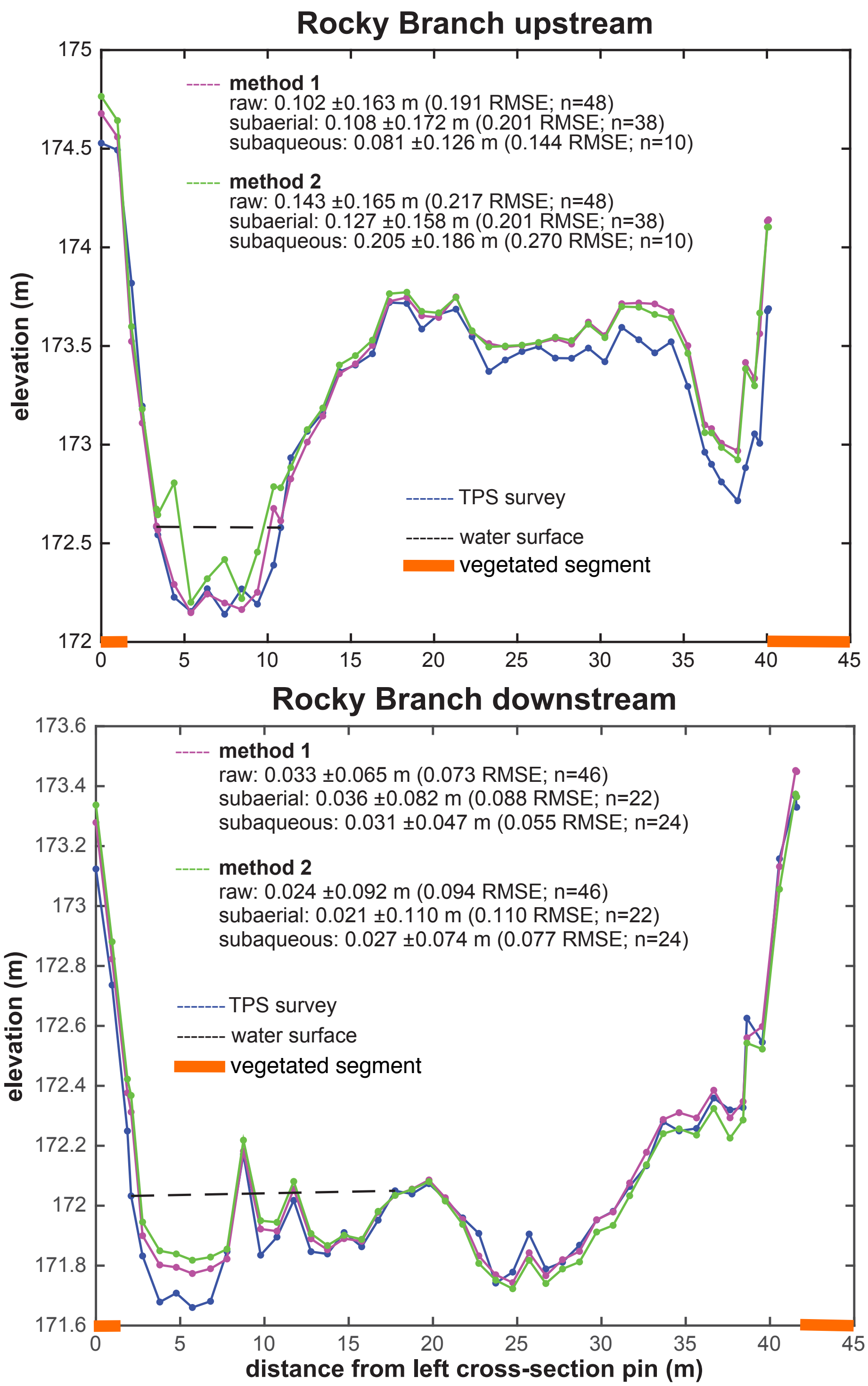

Figure 6. Comparison of cross-section profiles from the July 2014 combined sUAS SfM and TPS surveys on the Rocky Branch. Methods 1 and 2 are data georeferenced in Photoscan and CloudCompare, respectively. Orange lines highlight vegetated segments of cross sections for reference (not to scale).

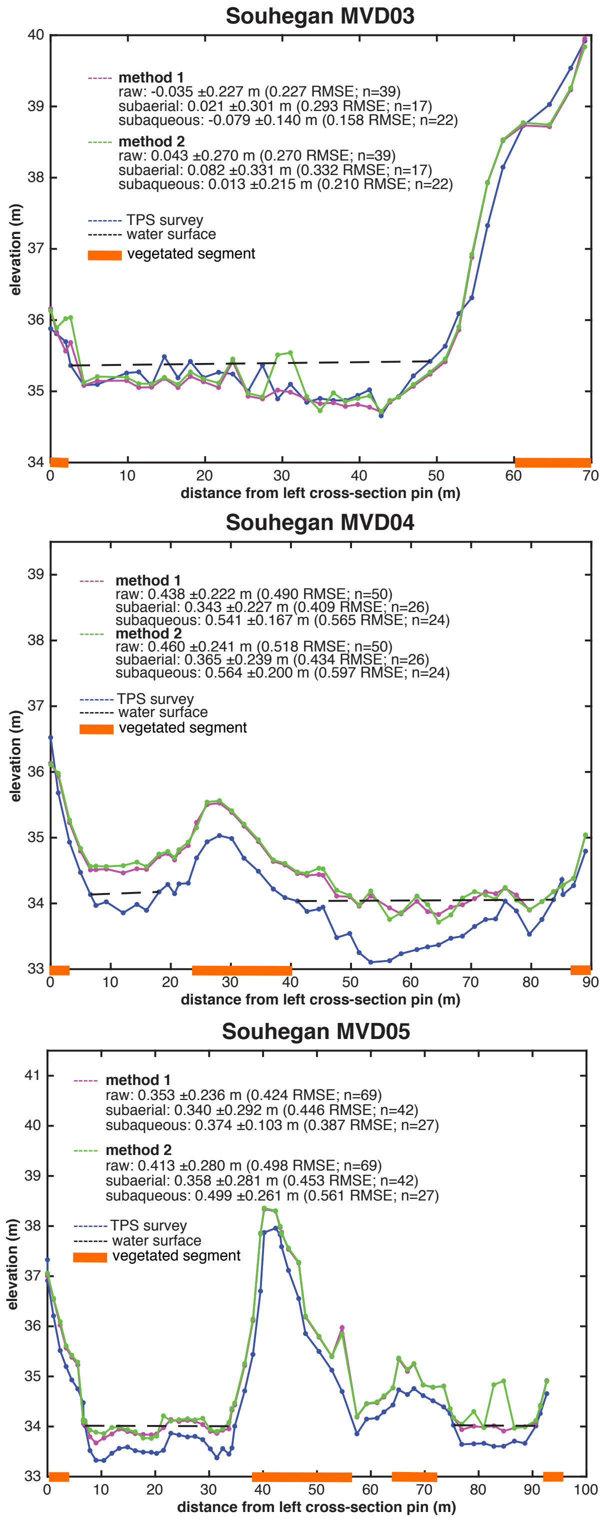

Figure 7. Comparison of cross-section profiles from the July 2014 combined sUAS SfM and TPS surveys on the Souhegan River. Methods 1 and 2 are data georeferenced in Photoscan and CloudCompare, respectively. Orange lines highlight vegetated segments of cross sections for reference (not to scale).

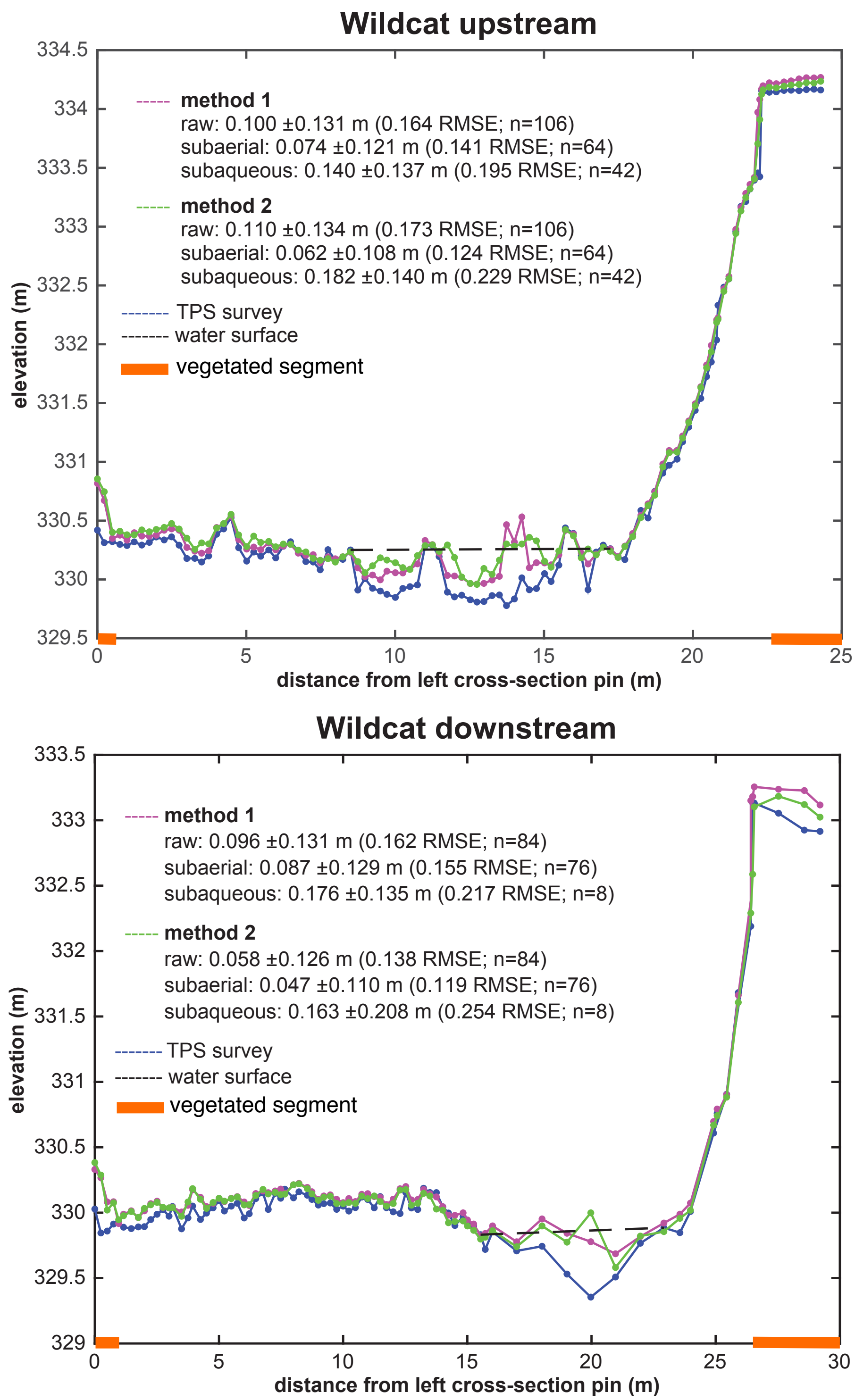

Figure 8. Comparison of cross-section profiles from the July 2014 combined sUAS SfM and TPS surveys on the Wildcat River. Methods 1 and 2 are data georeferenced in Photoscan and CloudCompare, respectively. Orange lines highlight vegetated segments of cross sections for reference (not to scale).

Table VIII. One-to-one point comparisons between sUAS SfM and TPS survey data (method 1)

		All points		Submerged points		Exposed points	
Survey site	Cross section; number of points, *n*	Average offset (ME) ±standard deviation (SD) (m)	RMSE (m)	Average offset (ME) ±standard deviation (SD) (m)	RMSE (m); number of points, *n*	Average offset (ME) ±standard deviation (SD) (m)	RMSE (m); number of points, *n*
Rocky Branch	Upstream cross section; 48	0.102 ±0.163	0.191	0.081 ±0.126	0.144; 10	0.108 ±0.172	0.201; 38
	Downstream cross section; 46	0.033 ±0.065	0.073	0.031 ±0.047	0.055; 24	0.036 ±0.082	0.088; 22
	Site-wide; 94	*0.069 ±0.129*	*0.145*				
Souhegan River	MVD03; 39	-0.035 ±0.227	0.227	-0.079 ±0.140	0.158; 22	0.021 ±0.301	0.293; 17
	MVD04; 50	0.438 ±0.222	0.408	0.541 ±0.167	0.565; 24	0.343 ±0.227	0.409; 26
	MVD05; 69	0.353 ±0.236	0.424	0.374 ±0.103	0.387; 27	0.340 ±0.292	0.446; 42
	Site-wide; 158	*0.284 ±0.295*	*0.409*				
Wildcat River	Upstream cross section; 106	0.100 ±0.131	0.164	0.140 ±0.137	0.195; 42	0.074 ±0.121	0.141; 64
	Downstream cross section; 84	0.096 ±0.131	0.162	0.176 ±0.135	0.217; 8	0.087 ±0.129	0.155; 76
	Site-wide; 190	*0.098 ±0.131*	*0.163*				
All sites; 442		***0.158 ±0.225***	***0.275***	**0.195 ±0.237**	**0.306; 156**	**0.137 ±0.217**	**0.256; 286**

RMSE = Root-mean-square-error

Measuring river geomorphic change

Geomorphic change detection (GCD) analysis comparing DEMs generated from sUAS SfM surveys in May 2015 and July 2014 at the Rocky Branch site and June 2014 to May 2015 at the Wildcat sites showed that minimal river channel change occurred on these river reaches during the year between surveys (Figure 9). Specifically, most of the cut bank at the Wildcat River site eroded 0-3 cm (with some areas eroding by 3-9 cm in the northern portion of this area) while 0-3 cm of deposition occurred on the point bar during the time between the 2014 and 2015 surveys. The riprapped cut bank at the Rocky Branch site aggraded by 0-3 cm and 0-3 cm of erosion happened in the mid-channel sediment (with some areas eroding by 3-6 cm in the southern portion of this area).

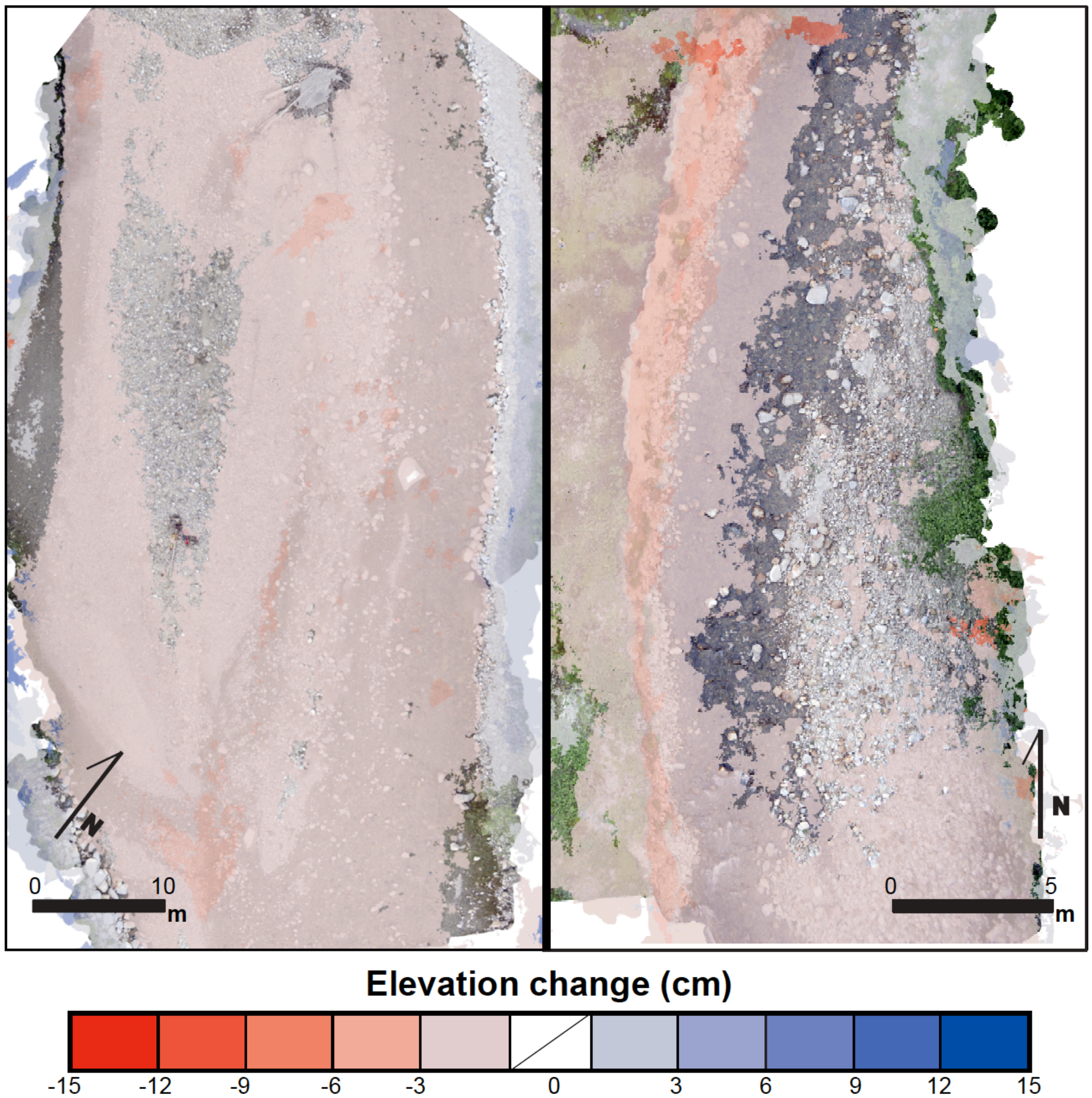

Figure 9. Maps showing results of GCD analysis (i.e. rates of erosion and deposition) at the Rocky Branch site from July 2014 to May 2015 (left) and Wildcat River study site from June 2014 to May 2015 (right)—the period between initial and final sUAS SfM surveys at the each. Blue indicates deposition whereas red shows erosion (after Wheaton et al. 2010). Base maps for both sites are orthoimages (with a resolution of ~1 cm per pixel) from their respective July 2014 sUAS SfM surveys.

Intrannual GCD analyses of the Wildcat River comparing sUAS SfM surveys from June 2014 to July 2014 and from July 2014 to May 2015 shows geomorphic change during these intervals that is smaller magnitude than the June 2014 to May 2015 analysis interval (Figure 10). In the June 2014 to July 2014 survey, erosion on the order of 0-3 cm occurred on the cut bank with areas of 0-3 deposition in areas scattered across the northern point bar. The July 2014 to May 2015 GCD analysis had similar results with 0-3 cm of erosion occurring on the cut bank, mid-channel sediment, and southern potion of the point bar as well as areas of 0-3 cm of deposition in areas scattered across the northern point bar.

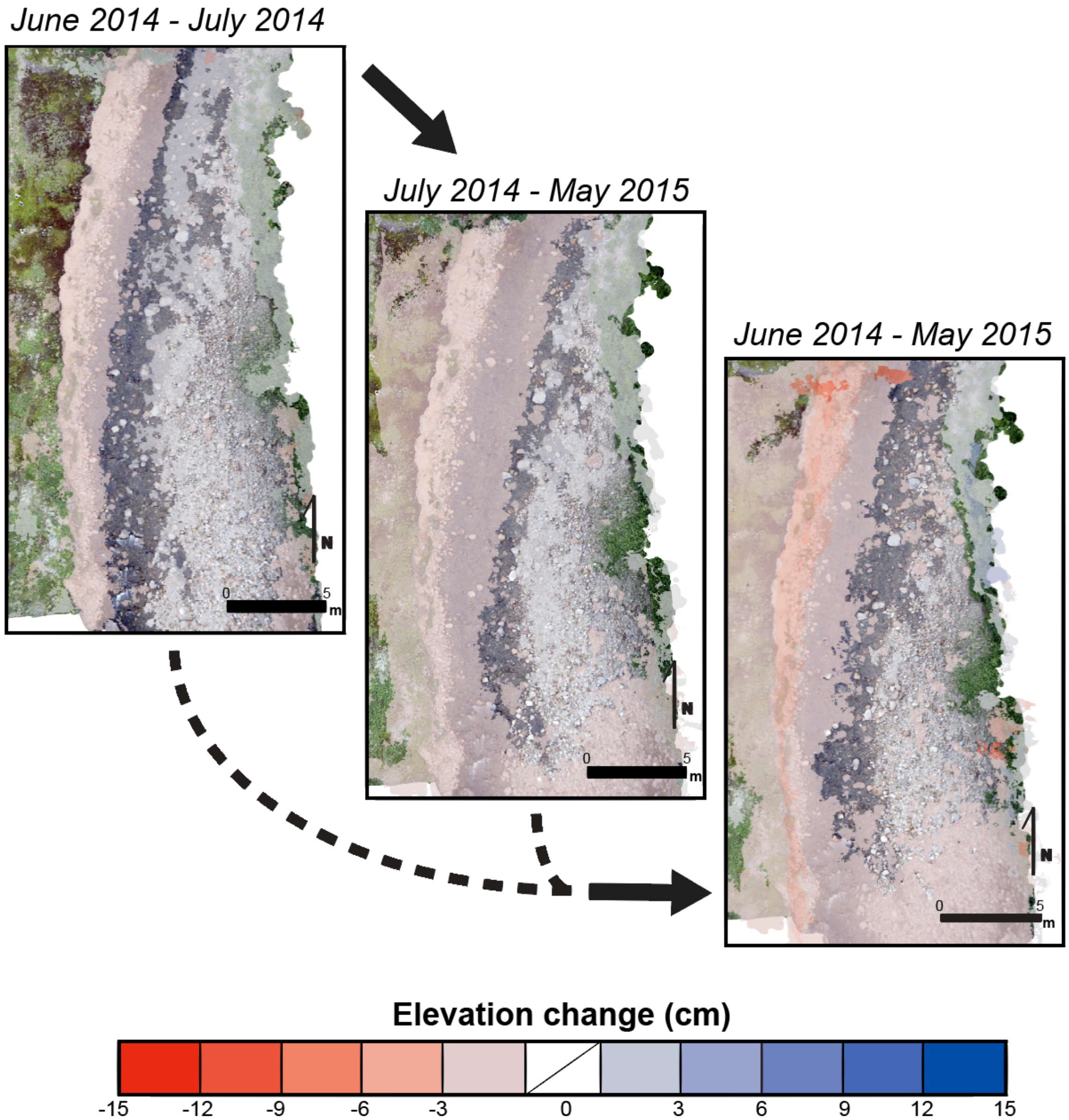

Figure 10. Maps showing results of GCD analysis (i.e. rates of erosion and deposition) at the Wildcat River study site from June 2014 to July 2014 (left), July 2014 to May 2015 (middle), and June 2014 to May 2015 (right). Blue indicates deposition whereas red shows erosion (after Wheaton et al. 2010). Base maps for both sites are orthoimages (with a resolution of ~1 cm per pixel) from their respective July 2014 sUAS SfM surveys.

Results summary

Airborne sUAS SfM surveys produced true color RGB orthoimagery and DEMs with ~1 cm pixel resolution (Figures 5 and 9). Uncertainties in TPS elevation measurement had baseline (OPUS-derived) horizontal and vertical measurement errors of ~1 ±0.5 cm and ~5 ±3 cm, respectively (Table V) as well as intrasurvey horizontal and vertical position errors of ~5 ±0.1 cm (Table VI). Although processing sUAS SfM surveys entirely within Photoscan is a less-biased, more accurate and precise workflow than integration of software external to Photoscan (i.e. CloudCompare), it outputs GCP elevations 0.2 ±20 cm higher than TPS inputs on average (with 20 cm RMSE; Table VII). One-to-one cross section comparisons show surveys using sUAS SfM systematically measure elevations ~15 ±25 cm higher than TPS (~0.30 cm RMSE; Figures 6-8; Table VIII). Interannual geomorphic change detection using sUAS SfM DEMs from the Rocky Branch and Wildcat sites show that little geomorphic change occurred in these river channels between the summers of 2014 and 2015, with the bulk of geomorphic change occurring due to a flood event in late June 2014 at the Wildcat site (Figures 9-10).

DISCUSSION

Data processing

Processing and georeferencing sUAS SfM data entirely with Photoscan software (Method 1) produced more accurate measurements than using external CloudCompare software to georeference sUAS SfM models produced in Photoscan (Method 2) in six of the seven total cross sections surveyed. Because Method 1 produced more accurate elevation measurements than Method 2 (Figures 6-8), I used only Method 1 for further error and geomorphic change detection analyses (Table VIII, Figures 9-10). The only cross sections where Method 2 produced more accurate elevation measurements than Method 1 was at the downstream cross section at the Wildcat site where Method 1 and 2 had RMSE values of 0.162 m and 0.138 m, respectively (Figure 8). This was an area where bathymetric surveys were obscured by riffles and it is possible that Method 2 could be better for resolving bathymetry in channels with more turbulent flow.

Another notable set of results was the downstream Rocky Branch cross section where Method 2 produced less biased elevation measurements that were closer to TPS measurements than Method 1, but were less accurate and precise. Whereas Method 1 measurements were 0.033 ±0.065 m with 0.073 RMSE, Method 2 produced 0.024 ±0.092 m with 0.094 RMSE. The better mean error result for this cross section indicated it is an artifact of noisy sUAS SfM data that happened to line up with the TPS data. As exemplified by the larger standard deviation and higher RMSE for Method 2 at this site, Method 2 generally is less accurate (higher RMSE) and less precise (greater SD) than Method 1 (Figures 6-8).

Bathymetry

Although sUAS SfM measurement errors were on the order of 10 cm across all sites (Table VIII), there are several distinct error trends within and between surveys. Perhaps the most obvious is that surveys measured by sUAS SfM were less accurate and precise at measuring submerged elevations than exposed topography. The notable exception to this rule was at the Rocky Branch site, where submerged data were actually more accurate than exposed data (but with a smaller sample size). The Rocky Branch was also the most accurate and precise sUAS SfM bathymetric survey and sUAS SfM elevations measured ~5 ±10 cm higher than TPS (10 cm RMSE), whereas the least accurate and precise bathymetric survey was at the Souhegan site where sUAS SfM elevations measured ~35 ±10 cm higher (30 cm RMSE) than TPS on average (Figures 6-8; Table VIII).

Because water refracts visible light and SfM uses this illumination to reconstruct depth, the submerged sUAS - TPS bias is greater than the exposed. Therefore, sUAS SfM measures shallower sections of river channels (e.g. MVD03 at the Souhegan site) more faithfully than deeper ones. Riffles like those at the Wildcat site increase surface opacity and limit SfM to reconstruct depth (the Rocky Branch site had less turbulent flow). Water turbidity also affects SfM sUAS survey results: more turbid water obstructs submerged sections of the river channel and prevents photogrammetric reconstruction therein. The Souhegan site had slightly more turbid water than the Rocky Branch and Wildcat sites, which may have contributed to less accurate results there (Tables VIII-IX).

Table IX. One-to-one point comparisons between sUAS SfM and TPS survey data for the Souhegan River site, classified by surface type

		All points		Submerged points		Exposed points	
Surface type classification (morphology or substrate)	Number of points, *n*	Average offset (ME) ±standard deviation (SD) (m)	RMSE (m)	Average offset (ME) ±standard deviation (SD) (m)	RMSE (m); number of points, *n*	Average offset (ME) ±standard deviation (SD) (m)	RMSE (m); number of points, *n*
Terrace (morphology)	22	*0.459 ±0.370*	*0.584*	-	-	-	-
Bank (morphology)	15	*0.136 ±0.294*	*0.315*	-	-	-	-
Riverbed (morphology)	121	*0.270 ±0.267*	*0.379*	0.292 ±0.289	0.410; 73	0.238 ±0.228	0.328; 48
Vegetated (substrate)	43	*0.364 ±0.324*	*0.484*	-	-	-	-
Cobble (substrate)	45	*0.049 ±0.266*	*0.267*	0.022 ±0.275	0.270; 26	0.085 ±0.256	0.263; 19
Sandy (substrate)	70	*0.387 ±0.196*	*0.433*	0.441 ±0.161	0.470; 47	0.274 ±0.215	0.346; 23

Spatially varying error in sUAS SfM surveys

Despite having precise and accurate coordinates from TPS surveys input into the PhotoScan SfM reconstruction during georeferencing (Tables V-VI), sUAS SfM surveys did not faithfully reproduce GCPs and errors in elevation measurement were spatially varying at all sites (Figures 6-8; Table VIII). Survey results were particularly poor at the Souhegan site, most likely due to sandy substrate that dominates the survey area (Tables VII-IX). The Souhegan site is also larger and had a lower concentration of GCPs than other the sites. However, preliminary analysis of a small set of GCP concentration metadata for all sites shows more survey area per GCP is not correlated (R^2=0.500; p=0.500) with higher survey error (Figure 11). Although ground control is important for producing an accurate sUAS SfM survey, other factors contributed to poor survey results.

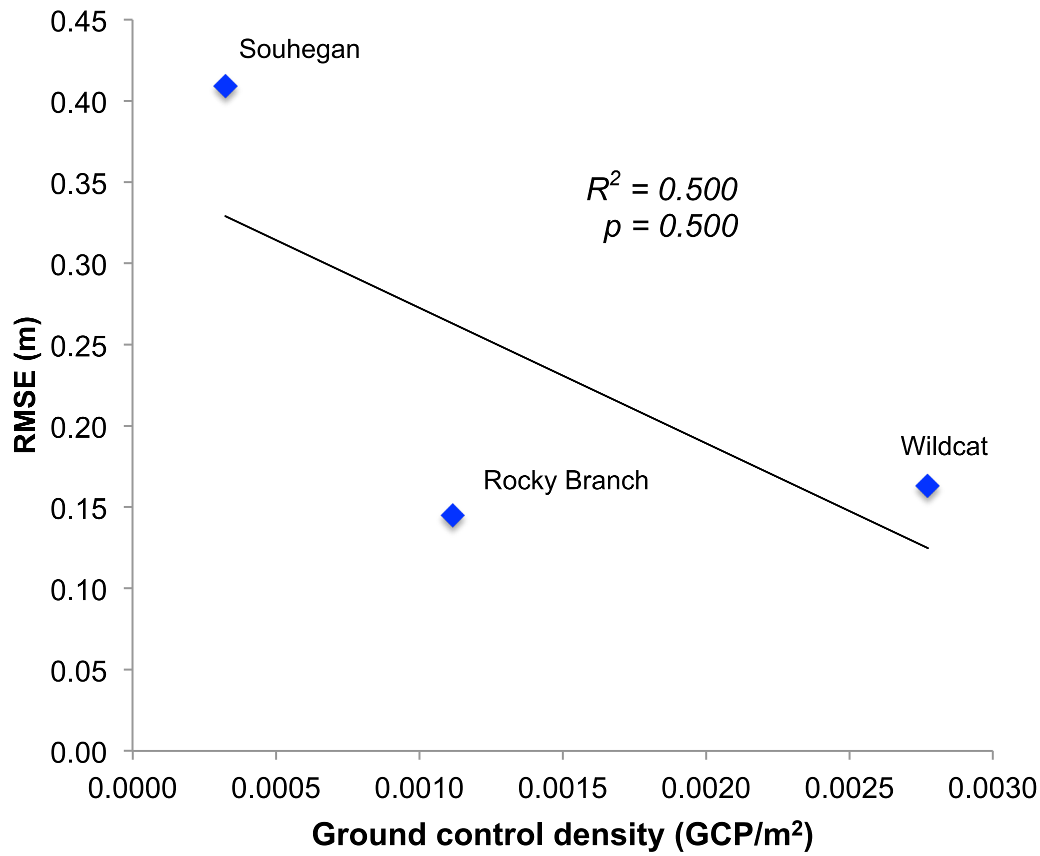

Figure 11. Relationship between ground control points placed throughout study sites and the accuracy of the resulting sUAS SfM survey (RMSE). Based on the three sites surveyed in this study, it appears that there is a modest relationship between ground control density and survey error.

Previous work focusing on concentric warping or “doming” of SfM surface reconstructions report systematic sUAS SfM survey errors whereby inconsistencies in surface elevation measurement are greater at the edges or center of the three dimensional model (James and Robson, 2014). Residual plots of all sUAS - TPS elevation measurements sites with respect to distance from the center of surveys from all three sites shows that there is a slight but significant (R^2=0.019; p=0.025) doming effect in the sUAS SfM surveys conducted in this study with greater errors at the edges of surveys than at their center (Figure 12). Decomposing this data by study site, the Rocky Branch (R^2=0.153; p=0.003) and Wildcat (R^2=0.141; p=0.001) sites show increasing measurement error toward survey edges whereas the Souhegan site (R^2=0.144; p=0.001) has increasing errors toward the survey center (Figure 12). Whereas the Rocky Branch and Wildcat sites appear to exhibit convex doming, the larger Souhegan shows concave doming. It appears that doming has a small but statistically significant effect on sUAS SfM survey error.

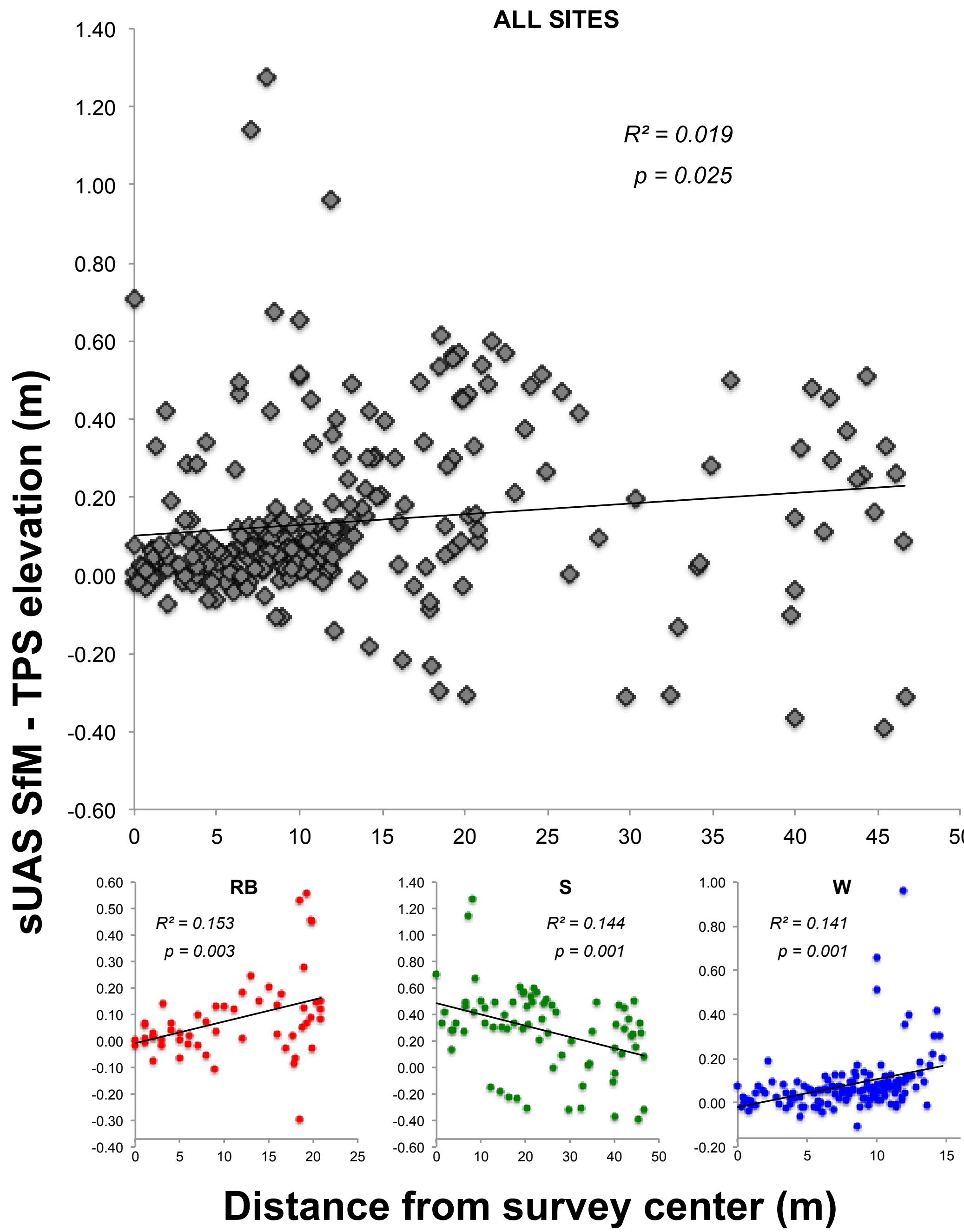

Figure 12. Differences in elevations measured my sUAS SfM and TPS surveys plotted against their distance from the center survey: [above] data from all sites and [below, l-r] from the Rocky Branch—RB (red), Souhegan—S (green) and Wildcat—W (blue) sites. There is a weak but significant correlation between error in sUAS elevation measurement and distance from survey center.

The TPS survey method allows for consistent measurement of bare earth elevation on vegetated surfaces. Because bare earth is usually obscured from aerial view by foliage in these areas, however, SfM reconstructions measure canopy height as elevation. Therefore, sUAS SfM measurements will be poorer than TPS at survey sites with more vegetation, such as river terraces or mid-channel islands. Although vegetation is restricted to the river floodplains and terraces at the Rocky Branch and Wildcat sites, the vegetated mid-channel island at the Souhegan site (particularly MVD05 in Figure 7), prevents accurate measurement of bare earth elevation. The doming observed at the Wildcat and Rocky Branch sites could actually be vegetation: larger survey errors at the edges of these sites could be errors related to increased canopy cover on the edge of these surveys (Figure 9).

A decomposition of survey results according to surface type at the Souhegan site reveals how the morphology and sedimentology of a surveyed area influenced the accuracy of the sUAS SfM measurements (Table IX). Vegetated portions of surveys produced less accurate results than those without vegetation (0.484 m RMSE). Point elevations on terraces (heavily vegetated) and located at the edges of survey areas,were measured less accurately (0.584 m RMSE) than those on banks (0.315 m RMSE) and riverbeds (0.379 m RMSE). Finally, cobble substrate produced better sUAS SfM survey results (0.267 m RMSE) than sandy substrate (0.433 m RMSE). It appears that the sandy substrate at the Souhegan site was an important contributor to the poor sUAS SfM survey results there; the Rocky Branch and Wildcat sites are gravel-bedded and produced more accurate sUAS SfM survey results than the Souhegan (Tables VIII-IX).

Similar to results of surveys at sites with shadows and vegetation, sites with a more uniform channel substrate such as sand in the Souhegan cross sections appears more difficult to reconstruct than the cobbles in the Rocky Branch and Wildcat sites. Because SfM relies on contrasting patterns of pixel values to execute pixel-matching algorithms, measure changes in perspective, and calculate depth, areas with channel sediment of uniform coloring and texture are more difficult to reconstruct (Table III; Figures 6-8). Finally, increased turbidity in the water column obscures channel bottom and limits the efficacy of SfM reconstructions. Orthoimagery indicates that the water column at the Souhegan is more turbid than the water at the other sites.

Comparison with previous studies

Initial surveys in this study produced high-resolution images that had error values consistent with similar work. Using similar data collection techniques and modes of comparison outlined here but without sUAS, Armistead (2013) found elevation values obtained using SfM to be 0.036 ±0.034 m higher than elevations measured with TPS on some of the same cross section in the Souhegan study area. These values are more accurate than the surveys conducted in this study, but the Armistead study used a higher-resolution digital single-lens reflex camera (DSLR) mounted on a 4.8-m pole. Others have performed SfM surveys of landscapes (also using higher-resolution cameras without sUAS) with RMSE values of 0.07 m (James and Robson, 2012), also much lower than those produced in this study.

This study has similar outcomes to others that specifically apply sUAS SfM to river channels (Table I). Studies of a site on a Canadian river using higher-resolution cameras and more expensive, autonomous sUAS (Tamminga et al., 2014; Tamminga et al., 2015) have lower RMSE values for both exposed (~0.05 m) and submerged (~0.10 m) surfaces of river channels than this study (~0.25 and 0.30 m RMSE, respectively; Table VIII). At sites located in the United Kingdom surveyed with a high-resolution camera and more expensive sUAS, Woodget et al. (2015) produced submerged and exposed measurement results of 0.044 and 0.064 m RMSE. In a study of a site in France using similar equipment to the Canadian surveys, Lejot et al. (2007) produced 0.02-0.040 m RMSE exposed survey results but were unable to resolve bathymetry. A survey completed with equipment similar to this study at a site in Finland measured exposed elevations with similar accuracy as this one but did not use SfM to measure bathymetry (Flener et al., 2013).

Perhaps the most notable aspect of this study is the relationship between the cost of sUAS SfM survey equipment and the resolution of the resulting elevation data (Table I). Although all river studies applying sUAS SfM produced elevation datasets with resolutions of 10 cm per pixel or better, this study reliably measured elevations and orthoimagery at a resolution of 1 cm per pixel or better, the best survey resolution result of work mentioned herein. Finally, these high-resolution data sets were acquired with equipment that cost around $1500 USD, $2000 less that the next most expensive sUAS SfM setup. Whereas some sUAS setups cost upwards of $50000, the results of this study are encouraging for those looking to produce detailed maps of fluvial environments with little investment in capital equipment.

sUAS SfM for GCD

Results of serial DEM comparison (GCD analysis) from sUAS SfM surveys conducted in May 2015 and July 2014 at the Rocky Branch and Wildcat sites fit well with models of river channel evolution (Figure 9). GCD classification rasters at the Rocky Branch site show 3-6 cm of overbank deposits and 0-9 cm of mid channel and cut bank erosion. At the Wildcat site, >10 cm of erosion occurred on the cut bank while 0-3 cm of deposition occurred on the point bar during the time between the July two surveys. Because the magnitude of geomorphic change at the Rocky Branch and Wildcat sites is less than the sUAS SfM error estimates, it should be noted that the GCD results are less than the accuracy estimate for sUAS SfM surveys (Table VIII) and GCD results are therefore within the margin of error for sUAS SfM surveys.

GCD results show consistent patterns of sediment transport between sites (Figures 9 and 10). There is deposition at the forested edges of the river corridor in both sites, particularly to the west at the Rocky Branch and to the east at the Wildcat. These differences probably reflect changes in vegetation height but could also be part of the doming effect. Lower-flow areas of both channels showed little geomorphic change (i.e. channel areas to the west and east of the Rocky Branch and Wildcat sites, respectively). Finally, the stationary boulders upon which GCPs were established at both sites exhibited only slight (if any) differences in elevation—meaning artificial GCD is small in magnitude.

In general, geomorphic change at the Rocky Branch and Wildcat sites are reasonable but fairly low in magnitude, making it difficult to separate GCD signal from noise. Serial comparison of orthoimagery from the sUAS shows transport of large (> 10 cm) clasts, confirming that sediment transport and therefore erosion and deposition were likely occurring in the channel in the time between surveys (Figure 13). Such geomorphic change was primarily a result of a flood event on June 26, 2014, which was the highest magnitude flow observed during the study period (Figure 11). GCD analysis of sUAS SfM survey results supports this observation, showing that a significant portion of the total geomorphic change at the Wildcat site from June 2014 to May 2015 occurred between the June 2014 and July 2014 surveys, an interval encapsulating the June 2014 flood event (Figure 10).

Ultimately, the interannual geomorphic change that occurred at the Rocky Branch and Wildcat sites was minimal and within the error envelope of sUAS SfM survey accuracy. Longer-term monitoring of these sites might capture more pronounced geomorphic change and better inform sUAS SfM as a tool for changes in fluvial geomorphology. Although orthoimages confirm active sediment transport at study sites during the study period, and corresponding GCD results appear reasonable, it remains difficult to determine real geomorphic change. The limited sampling size and time window make it challenging to separate actual geomorphic change from what might be just survey or method error.

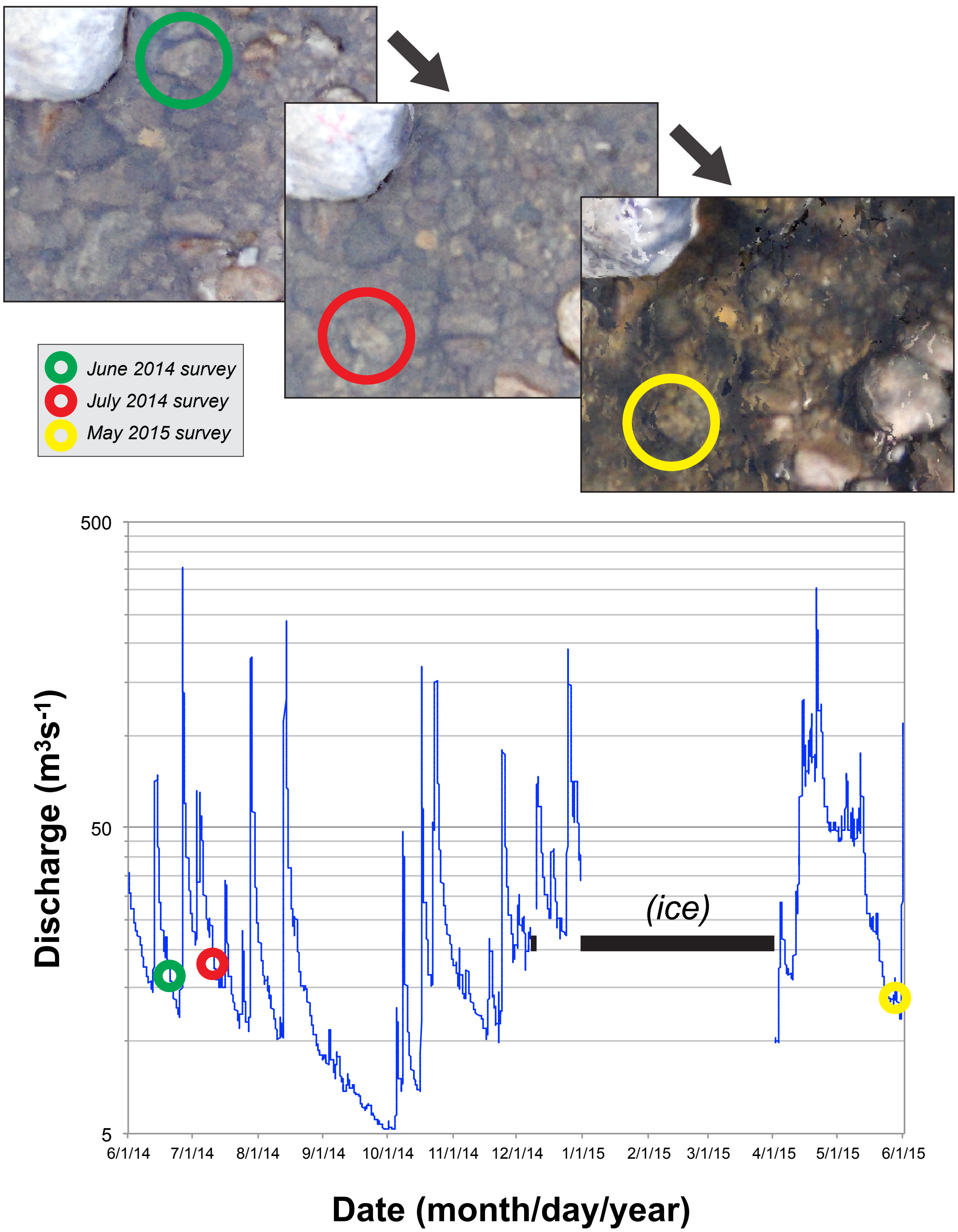

Figure 13. [above] Sediment transport at the Wildcat River site: the position of a ~10 cm cobble on June 25, 2014 (circled in green) and on July 14, 2014 (moved ~0.75 cm to position circled in red). This clast appears in the same position in imagery from the May 27, 2015 survey (yellow circle). [below] Discharge at the Saco River gauging station in Conway, NH from June 2014 to June 2015 (U.S. Geological Survey, 2015).

Camera position and lighting; future work

Several aspects of sUAS SfM survey parameters warrant further study. In particular, camera position geometry and lighting conditions appear to influence the resolution of sUAS SfM surveys (Table III). Traditional aerial photography designed for photogrammetry via stereoscopy uses photographs with the camera oriented normal to the land surface. The recommended architecture for SfM reconstruction, however, uses a convergent geometric construction for photography. Historically, aerial photographic surveys were conducted from fixed-wing aircraft that could not maneuver down close enough the ground surface to make convergent geometry practical. The maneuverability of sUAS quadcopters such as the one used in this study makes photography from multiple perspectives within a survey easy to accomplish.

Although the June 2015 surveys were convergent (Table III), the resolution of resulting data was not improved and, with no TPS measurements, it was not possible to assess accuracy. Because sUAS SfM relies on reflection of visible light, lighting conditions during sUAS SfM surveys could play a role in the quality of photogrammetry. Diffuse lighting conditions in the 2014 surveys could have produced higher resolution sUAS SfM datasets than the ones collected in direct sunlight during 2015. The effect of these and other variables on the survey data is difficult to determine based on this study alone, and should be examined further.

Applications

Aerial photograph surveys using sUAS serve an invaluable tool for those mapping habitat for sensitive species. Although U.S. Federal Aviation Administration (FAA) regulations prohibit unlicensed small aircraft from flying over 120 meters above the ground surface, the Phantom sUAS can easily be operated at this altitude within line-of-sight restrictions and provide high quality orthoimagery that can be quickly referenced using GPS systems. The ability of sUAS SfM surveys to map areas of active and intense restoration work can help monitor changes on a site to ensure proper execution of restoration plans.

Along with sUAS SfM, another emerging method for measuring river channel morphology is terrestrial lidar, also known as terrestrial laser scanning, or TLS (e.g., Bowen and Waltermire, 2002; Heritage and Hetherington, 2007; Milan et al., 2007). Using the same light reflection techniques as airborne lidar except from survey positions on the ground, terrestrial lidar generates a point cloud from a collection of feature points distributed across a surface. These points have assigned X, Y, and Z coordinates based on return times with respect to a fixed lidar survey station located with a high-precision global positioning system (GPS). The point cloud is then interpolated to create a DEM. Data acquisition is automatic and allows for measurement of tens of thousands of points per second with little human input.

TLS and sUAS SfM are fundamentally different methods for producing elevation datasets, with advantages and disadvantages in comparison to one another. TLS has an advantage over sUAS SfM in that it produces higher-resolution (~15 more points per 1

m^2 pixel), more accurate (~0.1 m lower elevation measurement error) datasets than sUAS SfM (Westoby et al., 2012). TLS also has the ability to penetrate vegetation (i.e. uniformly measure bare earth topography), whereas SfM does not. One disadvantage of TLS is that not all survey units are capable of producing RGB orthoimagery with one-to-one correspondence with elevation data. Perhaps the biggest difference between sUAS SfM and TLS surveys is that whereas sUAS SfM relies on external illumination (usually solar) to generate the visible light necessary for surveys, TLS must produce its own light necessary for surveys (coming directly from the TLS survey unit itself). Due to this limited illumination capacity, the extent of TLS surveys have inconsistencies in data coverage due to shadowing and the divergence of laser pulses as they radiate from the TLS unit.

TLS is ground-based and therefore an ideal method for surveying steep slopes because these surfaces are normal to instrumentation. Measuring landslides or other slope-driven geomorphic processes is an excellent application for TLS—especially in vegetated areas. However, sUAS, such as the one used in this study, are highly maneuverable and capable of collecting photographic data normal to steep faces. Ultimately, inconsistent data coverage, more laborious setup, limited maneuverability (always ground-based) and longer data acquisition time make TLS an inferior survey technique for larger sites (>0.01 km^2)—particularly in sparsely vegetated landscapes.

Currently, most areas around the world do not have high-resolution topographic data. Surveys with sUAS SfM may prove an ideal method for filling this gap as an alternative to airborne lidar, which requires considerable resources in terms of time and money. Airborne lidar elevation datasets are comparable with the sUAS SfM results presented here with respect to vertical accuracy, but lidar data has m-scale resolution whereas sUAS SfM DEMs have cm-scale resolution. The increased spatial topographic resolution of lidar (versus photogrammetric-based or satellite topography) has allowed researchers to quantitatively interrogate landscapes in a manner not previously possible (Roering et al., 2013). Because sUAS SfM surveys have higher resolution than lidar, they may permit study of smaller scale geomorphic processes such as the transport paths of individual particles. Furthermore, sUAS SfM does not survey as wide an area as airborne lidar, it is relatively inexpensive and can be deployed quickly and easily.

Preliminary results show aerial imagery and DEMs from sUAS SfM survey may prove useful in measuring short-term geomorphic change resulting from flood events. Recent public pleas by geomorphologists underscore the urgent need for widespread acquisition of high-resolution topographic datasets (Montgomery and Wartman, 2015). If effective, sUAS SfM would invigorate vital geomorphology research, land use planning, and natural disaster management throughout North America.

CONCLUSION

The sUAS SfM survey technique presented in this study consistently produced ~1 cm orthoimagery and DEMs (with an accuracy of ~25 cm) using a low cost sUAS survey instrument. Elevation data from these surveys were systematically higher than comparison with equivalent TPS measurements. Absolute GPS locations for TPS setups had accuracy (RMSE) of ~1 ±0.5 cm and 5 ±2.5 cm for horizontal and vertical positions, respectively; TPS measurements had accuracies of ~3 cm ±1 cm and ~4 cm ±1 cm for horizontal and vertical position, respectively. Although processing sUAS SfM surveys within Photoscan is a more accurate and precise workflow than external software (i.e. CloudCompare), it outputs GCP elevations 0.2 ±20 cm higher than TPS inputs on average (with 20 cm RMSE). Surveys using sUAS SfM measure elevations ~15 ±20 cm higher than TPS (~25 cm RMSE).

Interannual geomorphic change detection using sUAS SfM DEMs from the Rocky Branch and Wildcat sites show that little geomorphic change occurred in these river channels between the summers of 2014 and 2015. Because the magnitude of this change was small, it remains difficult to separate artificial from actual change at these sites. However, the overall patterns of change appear consistent with geomorphic expectations. Hydrologic data indicate that there were few high-magnitude flooding events during the study period and therefore the little geomorphic change would be expected to occur at the study sites. The largest flood event recorded during the study period (a flood with a magnitude just below that of a 2-year event) occurred between the June and July 2014 sUAS SfM surveys at the Wildcat site (which caused the most interannual geomorphic change, as shown by intrannual GCD analysis). Ideally, the effects of a larger, extreme flooding event would be evaluated using the sUAS SfM method outlined in this study.

Another particularly intriguing aspect of the study is sUAS SfM's ability to measure river channel bathymetry, a historically difficult surface to survey using methods other than TPS. Preliminary results indicate that sUAS SfM surveys are resolving submerged topography (0.306 m RMSE), albeit less accurately than exposed terrain (0.256 m RMSE). Survey results from smaller, relatively shallow, less turbid channels look especially promising. The bathymetric survey results in this study are similar to those found in other, more expensive sUAS SfM work and extend the applicability of sUAS as a topobathymetric measurement tool that is both more effective, less expensive and labor intensive than laser (lidar, TLS) and traditional survey measurements.

Professional land surveyors use highly accurate TPS measurements in order to create data used for land and river management across North America. TPS (or high-precision GPS) is a crucial aspect of the sUAS SfM protocol outlined herein, however, the addition of sUAS to traditional land survey methods shows how easily and affordably a vast amount of data can be added to a given survey. This study and others like it show the promise that sUAS SfM reconstructions hold for augmenting field surveying and mapping efforts. At very little cost (the DJI Phantom 2+ unit used in this study cost approximately USD $1500), land management strategies could be much better informed by high-resolution orthoimagery and DEMs. Here I show it is possible to set up a GCF in which a particular reach is outfitted with GCPs that are surveyed once and can be resurveyed and processed in quick succession as long as the GCPs within each scene remain consistent on an intrasurvey basis. Serial comparison of elevation and orthoimagery data from sUAS SfM surveys opens new avenues for landscape study.

ACKNOWLEDGEMENTS

Boston College supported this research through grants, fellowships, and capital equipment. I thank Noah Snyder, Seth Kruckenberg, and Gabrielle David for their guidance and assistance as well as Grace Lisius and Oluwaseun Fadugba for their help with data collection and processing.

I express much gratitude for my fellow Boston College Department of Earth and graduate students, particularly Aakash, Austin, Vanessa, Martha, Seun, Shaina, and Steve. Love to my friends and family for all their support along the way!

REFERENCES

Armistead, CC, 2013, Applications of 'Structure from Motion' Photogrammetry to River Channel Change Studies, Boston College Senior Undergraduate Thesis, Chestnut Hill, Massachusetts, USA, 68.

Babenroth, DL, and AN Strahler, 1945, Geomorphology and structure of the East Kaibab monocline, Arizona and Utah, *Geological Society of America Bulletin* 56(2), 107-150.

Bangen, SG, Wheaton, JM, Bouwes, N, Bouwes, B, and C Jordan, 2014, A methodological intercomparison of topographic survey techniques for characterizing wadeable streams and rivers, *Geomorphology* 206, 343-361.

Bowen, ZH, and RG Waltermire, 2002, Evaluation Of Light Detection And Ranging (LIDAR) For Measuring River Corridor Topography, *Journal of the American Water Resources Association* 38, 33-41.

Dietrich, WE, Wilson, CJ, Montgomery, DR, and J McKean, 1993, Analysis of Erosion Thresholds, Channel Networks, and Landscape Morphology Using a Digital Terrain Mode, *The Journal of Geology* 101, 259-278.

DJI Innovations, 2014, Your Flying Camera, Quadcopter Drone for Aerial Photography and Videography, http://www.dji.com/product/phantom-2-vision.

Eisenbeiss, H, Lambers, K, Sauerbier, M, and L Zhang, 2005, Photogrammetric documentation of an archaeological site (Palpa, Peru) using an autonomous model helicopter, *CIPA 2005,* 34.

Famiglietti, J, Lo, M, Ho, S, Bethune, J, Anderson, K, Syed, T, Swenson, S, de Linage, C, and M Rodell, 2011, Satellites measure recent rates of groundwater depletion in California's Central Valley, *Geophysical Research Letters* 38(3).

Farrington, A, 1928, The pre-glacial topography of the Liffey basin, *Proceedings of the Royal Irish Academy, Section B: Biological, Geological, and Chemical Science*, 148-170.

Flener, C, Vaaja, M, Jaakkola, A, Krooks, A, Kaartinen, H, Kukko, A, Kasvi, E, Hyyppä, H, Hyyppä, J, and O Alho, 2013, Seamless mapping of river channels at high resolution using mobile LiDAR and UAV-photography, *Remote Sensing* 5, 6382-6407.

Fonstad, MA, Dietrich, JT, Courville, BC, Jensen, JL, and PE Carbonneau, 2013, Topographic structure from motion: a new development in photogrammetric measurement, *Earth Surface Processes and Landforms* 38(4), 421-430.

Haugerud, RA, Harding, DJ, Johnson, SY, Harless, JL, Weaver, CS, and SL Sherrod, 2003, High-resolution lidar topography of the Puget Lowland, Washington*, GSA Today* 13(6), 4-10.

Heritage, G, and D Hetherington, 2007, Towards a protocol for laser scanning in fluvial geomorphology*, Earth Surface Processes and Landforms* 32(1), 66-74.

Hugemann, W, 2010, Correcting lens distortions in digital photographs*, Ingenieurbüro Morawski + Hugemann: Leverkusen, Germany*.

Hugenholtz, CH, Whitehead, K, Brown, OW, Barchyn, TE, Moorman, BJ, LeClair, A, Riddell K, and T Hamilton, 2013, Geomorphological mapping with a small unmanned aircraft system (sUAS): Feature detection and accuracy assessment of a photogrammetrically-derived digital terrain model*, Geomorphology* 194, 16-24.

James MR, and S Robson, 2014, Mitigating systematic error in topographic models derived from UAV and ground-based image networks*, Earth Surface Processes and Landforms* 39, 1413-1420.

James M, and S Robson, 2012, Straightforward reconstruction of 3D surfaces and topography with a camera: accuracy and geoscience application*, Journal of Geophysical Research: Earth Surface (2003-2012)* 117(F3).

Johnson, K, Nissen, E, Saripalli, S, Arrowsmith, JR, McGarey, P, Scharer, K, Williams, P, and K Blisniuk, 2014, Rapid mapping of ultrafine fault zone topography with structure from motion*, Geosphere* 10(5), 969-986.

Keim RF, Skaugset AE, and DS Bateman, 1999, Digital terrain modeling of small stream channels with a total-station theodolitw*, Advances in water resources* 23(1), 41-48.

Lane, S, Richards, K, and J Chandler, 1994, Developments in monitoring and modelling small-scale river bed topography*, Earth Surface Processes and Landforms* 19(4), 349-368.

Lejot, J, Delacourt, C, Piégay, H, Fournier, T, Trémélo, M, and P Allemand, 2007, Very high spatial resolution imagery for channel bathymetry and topography from an unmanned mapping controlled platform*, Earth Surface Processes and Landforms* 32(11), 1705-1725.

Merritts, DJ, Vincent, KR, and EE Wohl, 1994, Long river profiles, tectonism, and eustasy: a guide to interpreting fluvial terraces*, Journal of Geophysical Research* 99(B7), 14031-14050.

Milan, DJ, Heritage, GL, and D Hetherington D, 2007, Application of a 3D laser scanner in the assessment of erosion and deposition volumes and channel change in a proglacial river, *Earth surface processes and landforms* 32(11), 1657-1674.

Montgomery, DR, and E Foufoula-Georgiou, 1993, Channel network source representation using digital elevation models, *Water Resources Research* 29(12), 3925-3934.

Montgomery, DR, and J Wartman, March 21, 2015, How to Make Landslides Less Deadly, The New York Times.

Niethammer, U, James, M, Rothmund, S, Travelletti, J, and M Joswig, 2012, UAV-based remote sensing of the Super-Sauze landslide: Evaluation and results, *Engineering Geology* 128, 2-11.

Notebaert, B, Verstraeten, G, Govers, G, and J Poesen, 2009, Qualitative and quantitative applications of LiDAR imagery in fluvial geomorphology, *Earth Surface Processes and Landforms* 34(2), 217-231.

Pearson, AJ, Snyder, NP, and MJ Collins, 2011, Rates and processes of channel response to dam removal with a sand-filled impoundment, *Water Resources Research* 47(8).

Roering, JJ, Mackey, BH, Marshall, JA, Sweeney, KE, Deligne, NI, Booth, AM, Handwerger, AL, and C Cerovski-Darriau, 2013, 'You are HERE': Connecting the dots with airborne lidar for geomorphic fieldwork, *Geomorphology* 200, 172-183.

Snyder, NP, 2009, Studying stream morphology with airborne laser elevation data, *Eos, Transactions American Geophysical Union* 90(6), 45-46.

Stampone, MD, 2011, August 2011 Weather and Climate Summary, State of New Hampshire Department of Environmental Services.

stihl, 2014, GCP error low - high errors on DEM, Agisoft Community Forum, http://www.agisoft.com/forum/index.php?topic=2151.0.

Stone, W, 2006, The evolution of the National Geodetic Survey's continuously operating reference station network and online positioning user service, *Proceedings 2006 ION-IEEE Position, Location, and Navigation Symposium,* 25-27.

Strahler, AN, 1957, Quantitative analysis of watershed geomorphology, *Civ. Eng* 101, 1258-1262.

Tamminga, A, Hugenholtz, C, Eaton, B, and M Lapointe, 2014, Hyperspatial remote sensing of channel reach morphology and hydraulic fish habitat using an unmanned aerial vehicle (UAV): a first assessment in the context of river research and management, *River Research and Applications* 31(3), 379-391.

Tamminga, AD, Eaton, BC, and CH Hugenholtz, 2015, UAS-based remote sensing of fluvial change following an extreme flood event, *Earth Surface Processes and Landforms*.

Tonkin, T, Midgley, N, Graham, D, and J Labadz, 2014, The potential of small unmanned aircraft systems and structure-from-motion for topographic surveys: A test of emerging integrated approaches at Cwm Idwal, North Wales, *Geomorphology* 226.

U.S. Geological Survey, 2015, National Water Information System data available on the World Wide Web (Water Data for the Nation), http://waterdata.usgs.gov/nwis/.

Walther, BA, and JL Moore, 2005, The concepts of bias, precision and accuracy, and their use in testing the performance of species richness estimators, with a literature review of estimator performance, *Ecography* 28, 815-829.

Westoby, MJ, Brasington, J, Glasser, NF, Hambrey, MJ, and JM Reynolds, 2012, 'Structure-from-Motion'photogrammetry: A low-cost, effective tool for geoscience applications, *Geomorphology* 179, 300-314.

Wheaton, JM, Brasington, J, Darby, SE, and DA Sear, 2010, Accounting for uncertainty in DEMs from repeat topographic surveys: improved sediment budgets, *Earth Surface Processes and Landforms* 35(2), 136-156.

Wobus, C, Whipple, KX, Kirby, E, Snyder, N, Johnson, J, Spyropolou, K, Crosby, B, and D Sheehan, 2006, Tectonics from topography: Procedures, promise, and pitfalls. *Geological Society of America Special Papers* 398, 55-74.

Woodget, A, Carbonneau, P, Visser, F, and I Maddock, 2015, Quantifying submerged fluvial topography using hyperspatial resolution UAS imagery and structure from motion photogrammetry, *Earth Surface Processes and Landforms* 40, 47-64.

APPENDIX: OPUS REPORTS

(Rocky Branch, TPS station 1)

```
NGS OPUS-RS SOLUTION REPORT
                              ========================

All computed coordinate accuracies are listed as 1-sigma RMS values.
For additional information: http://www.ngs.noaa.gov/OPUS/about.jsp#accuracy

      USER: lucyc@bc.edu                             DATE: August 27, 2014
RINEX FILE: 1___196q.14o                             TIME: 18:39:51 UTC


  SOFTWARE: rsgps  1.37 RS90.prl 1.99.2             START: 2014/07/15 16:46:05
 EPHEMERIS: igs18012.eph [precise]                   STOP: 2014/07/15 17:25:55
  NAV FILE: brdc1960.14n                         OBS USED:  4923 /  5526   :  89%
  ANT NAME: LEIATX1230      NONE              QUALITY IND.  15.04/ 26.75
ARP HEIGHT: 1.842                          NORMALIZED RMS:        0.351


 REF FRAME: NAD_83(2011)(EPOCH:2010.0000)              IGS08 (EPOCH:2014.53620)

         X:      1478342.129(m)   0.009(m)          1478341.274(m)   0.009(m)
         Y:     -4342840.534(m)   0.012(m)         -4342839.124(m)   0.012(m)
         Z:      4416479.084(m)   0.007(m)          4416479.082(m)   0.007(m)

       LAT:   44  6 13.51177      0.005(m)        44  6 13.54804      0.005(m)
     E LON:  288 47 56.53609      0.007(m)       288 47 56.52013      0.007(m)
     W LON:   71 12  3.46391      0.007(m)        71 12  3.47987      0.007(m)
    EL HGT:          146.440(m)   0.015(m)               145.282(m)   0.015(m)
 ORTHO HGT:          173.619(m)   0.017(m) [NAVD88 (Computed using GEOID12A)]

                        UTM COORDINATES    STATE PLANE COORDINATES
                         UTM (Zone 19)         SPC (2800 NH  )
Northing (Y) [meters]     4885751.888          178274.305
Easting (X)  [meters]      323846.185          337286.000
Convergence  [degrees]    -1.53217393          0.32411533
Point Scale                0.99998165          0.99998376
Combined Factor            0.99995869          0.99996080

US NATIONAL GRID DESIGNATOR: 19TCJ2384685751(NAD 83)


                              BASE STATIONS USED
PID       DESIGNATION                        LATITUDE    LONGITUDE DISTANCE(m)
DO2056 MESP SOUTH PARIS CORS ARP          N441306.196 W0703047.107   56478.4
DL7764 P776 GUNSTOCKMRNH2008 CORS ARP     N433235.720 W0712242.789   63897.5
DK4107 VTD7 SAINT JOHNSBURY CORS ARP      N442352.310 W0720132.392   73529.7
DJ8957 VTOX BRADFORD CORS ARP             N440028.165 W0720651.609   73962.4
DO5451 MEGO GORHAM CORS ARP               N434052.067 W0702703.724   76394.0
DL3079 VTIP ISLAND POND CORS ARP          N444912.180 W0715325.838   96680.8
DL9078 NHCO NHDOT CONCORD CORS ARP        N431246.195 W0713111.475  102274.6
DO8675 BRU8 BRUNSWICK 8 CORS ARP          N435323.424 W0695648.026  103375.6
DM7840 VTHA HARDWICK CORS ARP             N443030.695 W0722157.163  103262.7

                 NEAREST NGS PUBLISHED CONTROL POINT
Information on nearest mark is not available due to database connectivity issues or
has restrictions on when or how it can be published.

This position and the above vector components were computed without any
knowledge by the National Geodetic Survey regarding the equipment or
field operating procedures used.
```

(Rocky Branch, TPS station 2)

```
NGS OPUS-RS SOLUTION REPORT
                              ========================

All computed coordinate accuracies are listed as 1-sigma RMS values.
For additional information: http://www.ngs.noaa.gov/OPUS/about.jsp#accuracy

      USER: lucyc@bc.edu                                DATE: August 27, 2014
RINEX FILE: 2___196s.14o                                TIME: 18:45:17 UTC


  SOFTWARE: rsgps  1.37 RS94.prl 1.99.2                START: 2014/07/15 18:02:35
 EPHEMERIS: igs18012.eph [precise]                      STOP: 2014/07/15 18:52:40
  NAV FILE: brdc1960.14n                            OBS USED:  5256 /  5528   :  95%
  ANT NAME: LEIATX1230      NONE                 QUALITY IND.  28.43/ 55.84
ARP HEIGHT: 1.814                             NORMALIZED RMS:        0.397


 REF FRAME: NAD_83(2011)(EPOCH:2010.0000)              IGS08 (EPOCH:2014.53635)

         X:      1478382.647(m)   0.012(m)           1478381.792(m)   0.012(m)
         Y:     -4342854.134(m)   0.018(m)          -4342852.724(m)   0.018(m)
         Z:      4416451.222(m)   0.021(m)           4416451.220(m)   0.021(m)

       LAT:   44  6 12.27887      0.004(m)        44  6 12.31513      0.004(m)
     E LON:  288 47 58.06361      0.009(m)       288 47 58.04765      0.009(m)
     W LON:   71 12  1.93639      0.009(m)        71 12  1.95235      0.009(m)
    EL HGT:          145.670(m)   0.029(m)               144.512(m)   0.029(m)
 ORTHO HGT:          172.851(m)   0.030(m) [NAVD88 (Computed using GEOID12A)]

                        UTM COORDINATES    STATE PLANE COORDINATES
                         UTM (Zone 19)         SPC (2800 NH  )
Northing (Y) [meters]     4885712.941          178236.445
Easting (X)  [meters]      323879.128          337320.188
Convergence  [degrees]    -1.53186895          0.32440864
Point Scale                0.99998150          0.99998379
Combined Factor            0.99995866          0.99996095

US NATIONAL GRID DESIGNATOR: 19TCJ2387985712(NAD 83)


                              BASE STATIONS USED
PID       DESIGNATION                        LATITUDE    LONGITUDE DISTANCE(m)
DO2056 MESP SOUTH PARIS CORS ARP           N441306.196 W0703047.107   56454.1
DL7764 P776 GUNSTOCKMRNH2008 CORS ARP      N433235.720 W0712242.789   63868.0
DK4107 VTD7 SAINT JOHNSBURY CORS ARP       N442352.310 W0720132.392   73577.2
DO5451 MEGO GORHAM CORS ARP                N434052.067 W0702703.724   76343.8
DL3079 VTIP ISLAND POND CORS ARP           N444912.180 W0715325.838   96731.4
DL9078 NHCO NHDOT CONCORD CORS ARP         N431246.195 W0713111.475  102246.4
DM7840 VTHA HARDWICK CORS ARP              N443030.695 W0722157.163  103310.0
DO8675 BRU8 BRUNSWICK 8 CORS ARP           N435323.424 W0695648.026  103334.0

                 NEAREST NGS PUBLISHED CONTROL POINT
Information on nearest mark is not available due to database connectivity issues or
has restrictions on when or how it can be published.

This position and the above vector components were computed without any
knowledge by the National Geodetic Survey regarding the equipment or
field operating procedures used.
```

(Saco, station 1)

```
 FILE: 1___1950.14o OP1409925473641

                              NGS OPUS-RS SOLUTION REPORT
                              ========================

All computed coordinate accuracies are listed as 1-sigma RMS values.
For additional information: http://www.ngs.noaa.gov/OPUS/about.jsp#accuracy

      USER: lucyc@bc.edu                          DATE: September 05, 2014
RINEX FILE: 1___195t.14o                          TIME: 14:06:14 UTC


  SOFTWARE: rsgps  1.37 RS92.prl 1.99.2          START: 2014/07/14 19:09:35
 EPHEMERIS: igs18011.eph [precise]                STOP: 2014/07/14 20:33:35
  NAV FILE: brdc1950.14n                      OBS USED:  6885 /  9036   :  76%
  ANT NAME: LEIATX1230      NONE             QUALITY IND.   5.93/ 59.45
ARP HEIGHT: 1.816                         NORMALIZED RMS:        0.448


 REF FRAME: NAD_83(2011)(EPOCH:2010.0000)            IGS08 (EPOCH:2014.53377)

         X:      1482361.961(m)   0.021(m)          1482361.106(m)   0.021(m)
         Y:     -4343964.283(m)   0.066(m)         -4343962.872(m)   0.066(m)
         Z:      4414005.590(m)   0.072(m)          4414005.588(m)   0.072(m)

       LAT:   44  4 22.74208      0.011(m)        44  4 22.77835      0.011(m)
     E LON:  288 50 31.27157      0.007(m)       288 50 31.25568      0.007(m)
     W LON:   71  9 28.72843      0.007(m)        71  9 28.74432      0.007(m)
    EL HGT:          120.923(m)   0.099(m)               119.764(m)   0.099(m)
 ORTHO HGT:          148.189(m)   0.100(m) [NAVD88 (Computed using GEOID12A)]

                        UTM COORDINATES    STATE PLANE COORDINATES
                         UTM (Zone 19)         SPC (2800 NH  )
Northing (Y) [meters]     4882243.153          174875.875
Easting (X)  [meters]      327196.703          340748.424
Convergence  [degrees]    -1.50140536          0.35383404
Point Scale                0.99996727          0.99998708
Combined Factor            0.99994831          0.99996812

US NATIONAL GRID DESIGNATOR: 19TCJ2719682243(NAD 83)


                              BASE STATIONS USED
PID       DESIGNATION                        LATITUDE    LONGITUDE DISTANCE(m)
DO2056 MESP SOUTH PARIS CORS ARP           N441306.196 W0703047.107   54068.8
DL7764 P776 GUNSTOCKMRNH2008 CORS ARP      N433235.720 W0712242.789   61478.6
DO5451 MEGO GORHAM CORS ARP                N434052.067 W0702703.724   71582.2
DJ8957 VTOX BRADFORD CORS ARP              N440028.165 W0720651.609   76995.3
DK4107 VTD7 SAINT JOHNSBURY CORS ARP       N442352.310 W0720132.392   78155.4
AJ2693 YMTS MTS YARMOUTH COOP CORS ARP     N434754.608 W0701120.297   83567.8
DL9078 NHCO NHDOT CONCORD CORS ARP         N431246.195 W0713111.475   99928.6
DL3079 VTIP ISLAND POND CORS ARP           N444912.180 W0715325.838  101449.5
DI1075 NHUN U NEW HAMPSHIRE CORS ARP       N430833.179 W0705706.862  104705.5

                 NEAREST NGS PUBLISHED CONTROL POINT
Information on nearest mark is not available due to database connectivity issues or
has restrictions on when or how it can be published.

This position and the above vector components were computed without any
knowledge by the National Geodetic Survey regarding the equipment or
field operating procedures used.
```

(Saco, TPS station 2)

```
FILE: 82__1950.14o OP1409924801169

                              NGS OPUS-RS SOLUTION REPORT
                              ========================

All computed coordinate accuracies are listed as 1-sigma RMS values.
For additional information: http://www.ngs.noaa.gov/OPUS/about.jsp#accuracy

      USER: lucyc@bc.edu                              DATE: September 05, 2014
RINEX FILE: 82__195v.14o                              TIME: 13:54:00 UTC


  SOFTWARE: rsgps  1.37 RS91.prl 1.99.2              START: 2014/07/14 21:05:35
 EPHEMERIS: igs18011.eph [precise]                    STOP: 2014/07/14 22:23:00
  NAV FILE: brdc1950.14n                          OBS USED:  4590 /  8604   :  53%
  ANT NAME: LEIATX1230      NONE               QUALITY IND.  14.51/  8.07
ARP HEIGHT: 1.865                           NORMALIZED RMS:        0.468


 REF FRAME: NAD_83(2011)(EPOCH:2010.0000)              IGS08 (EPOCH:2014.53399)

         X:      1482195.808(m)   0.013(m)           1482194.953(m)   0.013(m)
         Y:     -4344000.414(m)   0.017(m)          -4343999.003(m)   0.017(m)
         Z:      4414026.745(m)   0.017(m)           4414026.743(m)   0.017(m)

       LAT:   44  4 23.67311      0.006(m)        44  4 23.70938      0.006(m)
     E LON:  288 50 23.68059      0.008(m)       288 50 23.66470      0.008(m)
     W LON:   71  9 36.31941      0.008(m)        71  9 36.33530      0.008(m)
    EL HGT:          121.655(m)   0.026(m)               120.496(m)   0.026(m)
 ORTHO HGT:          148.919(m)   0.027(m) [NAVD88 (Computed using GEOID12A)]

                        UTM COORDINATES    STATE PLANE COORDINATES
                         UTM (Zone 19)         SPC (2800 NH  )
Northing (Y) [meters]     4882276.306           174903.569
Easting (X)  [meters]      327028.605           340579.337
Convergence  [degrees]    -1.50288014           0.35236893
Point Scale                0.99996798           0.99998691
Combined Factor            0.99994890           0.99996783

US NATIONAL GRID DESIGNATOR: 19TCJ2702882276(NAD 83)


                              BASE STATIONS USED
PID       DESIGNATION                        LATITUDE    LONGITUDE DISTANCE(m)
DO2056 MESP SOUTH PARIS CORS ARP          N441306.196 W0703047.107   54221.2
DL7764 P776 GUNSTOCKMRNH2008 CORS ARP     N433235.720 W0712242.789   61457.4
DO5451 MEGO GORHAM CORS ARP               N434052.067 W0702703.724   71734.1
DJ8957 VTOX BRADFORD CORS ARP             N440028.165 W0720651.609   76829.6
DK4107 VTD7 SAINT JOHNSBURY CORS ARP      N442352.310 W0720132.392   77992.6
AJ2693 YMTS MTS YARMOUTH COOP CORS ARP    N434754.608 W0701120.297   83735.8
DL9078 NHCO NHDOT CONCORD CORS ARP        N431246.195 W0713111.475   99906.5
DL3079 VTIP ISLAND POND CORS ARP          N444912.180 W0715325.838  101329.5
DI1075 NHUN U NEW HAMPSHIRE CORS ARP      N430833.179 W0705706.862  104761.1

                 NEAREST NGS PUBLISHED CONTROL POINT
Information on nearest mark is not available due to database connectivity issues or
has restrictions on when or how it can be published.

This position and the above vector components were computed without any
knowledge by the National Geodetic Survey regarding the equipment or
field operating procedures used.
```

(Souhegan, TPS station 1)

```
NGS OPUS-RS SOLUTION REPORT
                              ========================

All computed coordinate accuracies are listed as 1-sigma RMS values.
For additional information: http://www.ngs.noaa.gov/OPUS/about.jsp#accuracy

      USER: lucyc@bc.edu                              DATE: August 27, 2014
RINEX FILE: 1___202o.14o                              TIME: 11:46:55 UTC


  SOFTWARE: rsgps  1.37 RS93.prl 1.99.2              START: 2014/07/21 14:15:05
 EPHEMERIS: igs18021.eph [precise]                    STOP: 2014/07/21 16:00:35
  NAV FILE: brdc2020.14n                          OBS USED: 10755 / 11745    :  92%
  ANT NAME: LEIATX1230      NONE                QUALITY IND.  63.05/130.32
ARP HEIGHT: 1.760                            NORMALIZED RMS:        0.319


 REF FRAME: NAD_83(2011)(EPOCH:2010.0000)              IGS08 (EPOCH:2014.55241)

         X:      1486257.087(m)   0.005(m)          1486256.238(m)   0.005(m)
         Y:     -4440553.683(m)   0.013(m)         -4440552.259(m)   0.013(m)
         Z:      4315987.327(m)   0.011(m)          4315987.313(m)   0.011(m)

       LAT:   42 51 30.07535      0.004(m)        42 51 30.11073      0.004(m)
     E LON:  288 30 19.57482      0.004(m)       288 30 19.55926      0.004(m)
     W LON:   71 29 40.42518      0.004(m)        71 29 40.44074      0.004(m)
    EL HGT:           10.472(m)   0.016(m)                9.275(m)   0.016(m)
 ORTHO HGT:           38.016(m)   0.019(m) [NAVD88 (Computed using GEOID12A)]

                        UTM COORDINATES    STATE PLANE COORDINATES
                         UTM (Zone 19)         SPC (2800 NH  )
Northing (Y) [meters]     4748104.148           39821.359
Easting (X)  [meters]      296200.970          314065.262
Convergence  [degrees]    -1.69735461          0.11706339
Point Scale                1.00011100          0.99996910
Combined Factor            1.00010936          0.99996746

US NATIONAL GRID DESIGNATOR: 19TBH9620048104(NAD 83)


                              BASE STATIONS USED
PID       DESIGNATION                        LATITUDE    LONGITUDE DISTANCE(m)
DI1075 NHUN U NEW HAMPSHIRE CORS ARP       N430833.179 W0705706.862   54357.0
DI0964 FMTS MTS FRAM COOP CORS ARP         N421800.171 W0712630.865   62169.7
DL7764 P776 GUNSTOCKMRNH2008 CORS ARP      N433235.720 W0712242.789   76676.1
DP1320 MABN BERNARDSTON CORS ARP           N424011.991 W0723228.643   88194.3
DI0966 XMTS MTS FOX COOP CORS ARP          N420350.018 W0711501.669   90505.1
DJ8961 VTSP SPRINGFIELD VT CORS ARP        N431653.241 W0722839.238   92841.6
DP1959 MASB STURBRIDGE CORS ARP            N420641.081 W0720513.985   96222.4
DE8093 HAMP NORTHAMPTON CORS ARP           N421903.872 W0723822.403  111530.6
DO9471 MAPL PLYMOUTH CORS ARP              N415619.314 W0703918.243  123338.0

                 NEAREST NGS PUBLISHED CONTROL POINT
Information on nearest mark is not available due to database connectivity issues or
has restrictions on when or how it can be published.

This position and the above vector components were computed without any
knowledge by the National Geodetic Survey regarding the equipment or
field operating procedures used.
```

(Souhegan, TPS station 2)

```
 NGS OPUS SOLUTION REPORT
                             ========================

All computed coordinate accuracies are listed as peak-to-peak values.
For additional information: http://www.ngs.noaa.gov/OPUS/about.jsp#accuracy

      USER: lucyc@bc.edu                          DATE: August 27, 2014
RINEX FILE: 102_202q.14o                          TIME: 11:42:46 UTC


  SOFTWARE: page5  1209.04 master92.pl 022814      START: 2014/07/21  16:18:00
 EPHEMERIS: igs18021.eph [precise]                 STOP: 2014/07/21  18:45:00
  NAV FILE: brdc2020.14n                       OBS USED:  6185 /  6372   :  97%
  ANT NAME: LEIATX1230      NONE             # FIXED AMB:    31 /    32   :  97%
ARP HEIGHT: 1.803                            OVERALL RMS: 0.013(m)


 REF FRAME: NAD_83(2011)(EPOCH:2010.0000)             IGS08 (EPOCH:2014.5527)

         X:      1486213.713(m)   0.011(m)          1486212.864(m)   0.011(m)
         Y:     -4440581.636(m)   0.023(m)         -4440580.212(m)   0.023(m)
         Z:      4315969.004(m)   0.017(m)          4315968.990(m)   0.017(m)

       LAT:   42 51 29.35925      0.004(m)        42 51 29.39462      0.004(m)
     E LON:  288 30 17.37225      0.014(m)       288 30 17.35669      0.014(m)
     W LON:   71 29 42.62775      0.014(m)        71 29 42.64331      0.014(m)
    EL HGT:            7.349(m)   0.026(m)                 6.152(m)   0.026(m)
 ORTHO HGT:           34.894(m)   0.044(m) [NAVD88 (Computed using GEOID12A)]

                        UTM COORDINATES    STATE PLANE COORDINATES
                         UTM (Zone 19)         SPC (2800 NH  )
Northing (Y)  [meters]    4748083.539           39799.160
Easting (X)   [meters]     296150.329          314015.305
Convergence   [degrees]   -1.69776485          0.11664679
Point Scale                1.00011125          0.99996908
Combined Factor            1.00011010          0.99996793

US NATIONAL GRID DESIGNATOR: 19TBH9615048083(NAD 83)


                             BASE STATIONS USED
PID       DESIGNATION                        LATITUDE    LONGITUDE DISTANCE(m)
DP1961 MAWM WESTMINSTER CORS ARP           N423340.621 W0715559.207   48733.8
DF9215 ZBW1 BOSTON WAAS 1 CORS ARP         N424408.558 W0712849.518   13655.8
DL9078 NHCO NHDOT CONCORD CORS ARP         N431246.195 W0713111.475   39453.9

                 NEAREST NGS PUBLISHED CONTROL POINT
MY0421      A 10                           N425141.5   W0712915.2       726.2

This position and the above vector components were computed without any
knowledge by the National Geodetic Survey regarding the equipment or
field operating procedures used.
```

(Wildcat, TPS station 1)

```
NGS OPUS-RS SOLUTION REPORT
                              ========================

All computed coordinate accuracies are listed as 1-sigma RMS values.
For additional information: http://www.ngs.noaa.gov/OPUS/about.jsp#accuracy

      USER: lucyc@bc.edu                           DATE: August 27, 2014
RINEX FILE: 1___196m.14o                           TIME: 18:26:49 UTC


  SOFTWARE: rsgps  1.37 RS50.prl 1.99.2           START: 2014/07/15 12:12:05
 EPHEMERIS: igs18012.eph [precise]                 STOP: 2014/07/15 13:51:55
  NAV FILE: brdc1960.14n                       OBS USED:  7209 / 10152   :  71%
  ANT NAME: LEIATX1230      NONE            QUALITY IND.  26.17/ 57.79
ARP HEIGHT: 1.830                       NORMALIZED RMS:        0.365


 REF FRAME: NAD_83(2011)(EPOCH:2010.0000)              IGS08 (EPOCH:2014.53573)

         X:      1476753.495(m)   0.009(m)          1476752.640(m)   0.009(m)
         Y:     -4336598.919(m)   0.022(m)         -4336597.510(m)   0.022(m)
         Z:      4423326.098(m)   0.023(m)          4423326.097(m)   0.023(m)

       LAT:   44 11 17.56554      0.004(m)        44 11 17.60186      0.004(m)
     E LON:  288 48 19.38485      0.005(m)       288 48 19.36886      0.005(m)
     W LON:   71 11 40.61515      0.005(m)        71 11 40.63114      0.005(m)
    EL HGT:          308.122(m)   0.033(m)               306.967(m)   0.033(m)
 ORTHO HGT:          334.964(m)   0.034(m) [NAVD88 (Computed using GEOID12A)]

                        UTM COORDINATES    STATE PLANE COORDINATES
                         UTM (Zone 19)         SPC (2800 NH  )
Northing (Y) [meters]     4895119.493           187661.608
Easting (X)  [meters]      324604.557           337740.304
Convergence  [degrees]    -1.53007421           0.32903196
Point Scale                0.99997836           0.99998418
Combined Factor            0.99993005           0.99993587

US NATIONAL GRID DESIGNATOR: 19TCJ2460495119(NAD 83)


                              BASE STATIONS USED
PID       DESIGNATION                        LATITUDE    LONGITUDE DISTANCE(m)
DO2056 MESP SOUTH PARIS CORS ARP          N441306.196 W0703047.107   54580.8
DK4107 VTD7 SAINT JOHNSBURY CORS ARP      N442352.310 W0720132.392   70300.6
DL7764 P776 GUNSTOCKMRNH2008 CORS ARP     N433235.720 W0712242.789   73174.7
DJ8957 VTOX BRADFORD CORS ARP             N440028.165 W0720651.609   76326.5
DO5451 MEGO GORHAM CORS ARP               N434052.067 W0702703.724   82094.1
DL3079 VTIP ISLAND POND CORS ARP          N444912.180 W0715325.838   89401.9
AJ2693 YMTS MTS YARMOUTH COOP CORS ARP    N434754.608 W0701120.297   91556.1
DO2873 MERA RANGELEY CORS ARP             N445825.333 W0703910.583   97316.7
DM7840 VTHA HARDWICK CORS ARP             N443030.695 W0722157.163   99946.1

                 NEAREST NGS PUBLISHED CONTROL POINT
Information on nearest mark is not available due to database connectivity issues or
has restrictions on when or how it can be published.

This position and the above vector components were computed without any
knowledge by the National Geodetic Survey regarding the equipment or
field operating procedures used.
```

(Wildcat, TPS station 2)

```
NGS OPUS-RS SOLUTION REPORT
                              ========================

All computed coordinate accuracies are listed as 1-sigma RMS values.
For additional information: http://www.ngs.noaa.gov/OPUS/about.jsp#accuracy

      USER: lucyc@bc.edu                           DATE: August 27, 2014
RINEX FILE: 2___196o.14o                           TIME: 18:26:51 UTC


  SOFTWARE: rsgps  1.37 RS52.prl 1.99.2           START: 2014/07/15 14:00:15
 EPHEMERIS: igs18012.eph [precise]                 STOP: 2014/07/15 15:45:35
  NAV FILE: brdc1960.14n                       OBS USED:  7857 / 10701   :  73%
  ANT NAME: LEIATX1230      NONE            QUALITY IND.  37.56/100.60
ARP HEIGHT: 1.775                        NORMALIZED RMS:        0.317


 REF FRAME: NAD_83(2011)(EPOCH:2010.0000)              IGS08 (EPOCH:2014.53595)

        X:      1476755.338(m)   0.007(m)          1476754.483(m)   0.007(m)
        Y:     -4336611.902(m)   0.008(m)         -4336610.493(m)   0.008(m)
        Z:      4423311.418(m)   0.009(m)          4423311.417(m)   0.009(m)

      LAT:   44 11 16.93358      0.004(m)        44 11 16.96990      0.004(m)
    E LON:  288 48 19.27497      0.005(m)       288 48 19.25897      0.005(m)
    W LON:   71 11 40.72503      0.005(m)        71 11 40.74103      0.005(m)
   EL HGT:          307.128(m)   0.012(m)               305.973(m)   0.012(m)
 ORTHO HGT:          333.971(m)   0.015(m) [NAVD88 (Computed using GEOID12A)]

                        UTM COORDINATES    STATE PLANE COORDINATES
                         UTM (Zone 19)         SPC (2800 NH  )
Northing (Y) [meters]     4895100.060           187642.089
Easting (X)  [meters]      324601.597           337737.975
Convergence  [degrees]    -1.53009068           0.32900965
Point Scale                0.99997837           0.99998417
Combined Factor            0.99993022           0.99993601

US NATIONAL GRID DESIGNATOR: 19TCJ2460195100(NAD 83)


                              BASE STATIONS USED
PID       DESIGNATION                        LATITUDE    LONGITUDE DISTANCE(m)
DO2056 MESP SOUTH PARIS CORS ARP          N441306.196 W0703047.107   54584.5
DK4107 VTD7 SAINT JOHNSBURY CORS ARP      N442352.310 W0720132.392   70304.8
DL7764 P776 GUNSTOCKMRNH2008 CORS ARP     N433235.720 W0712242.789   73155.1
DJ8957 VTOX BRADFORD CORS ARP             N440028.165 W0720651.609   76319.1
DO5451 MEGO GORHAM CORS ARP               N434052.067 W0702703.724   82082.6
DL3079 VTIP ISLAND POND CORS ARP          N444912.180 W0715325.838   89415.8
AJ2693 YMTS MTS YARMOUTH COOP CORS ARP    N434754.608 W0701120.297   91549.1
DN9934 MEFR FARMINGTON CORS ARP           N444028.974 W0700754.542  100430.8
DM7840 VTHA HARDWICK CORS ARP             N443030.695 W0722157.163   99950.8

                 NEAREST NGS PUBLISHED CONTROL POINT
Information on nearest mark is not available due to database connectivity issues or
has restrictions on when or how it can be published.

This position and the above vector components were computed without any
knowledge by the National Geodetic Survey regarding the equipment or
field operating procedures used.
```